

We thank the referees for their valuable comments. We respond below each comment in blue highlighted text and indicate the corresponding changes to the manuscript where relevant.

Anonymous Referee #1

General comments

This manuscript describes laboratory experiments using the Filter Inlet for Gases and Aerosols/Chemical Ionization Mass Spectrometry (FIGAERO-CIMS) technique that aim to investigate the nature of the components of IEPOX-derived secondary organic aerosol (IEPOX-SOA). Specifically, the work addresses the inconsistency between GCMS approaches that have identified semi-volatile molecular components and volatility measurements that have indicated that the bulk of IEPOX-SOA must be made up of much lower volatility molecular components. The main claim is that a desorption signal that corresponds to $C_5H_{12}O_4$ has two maxima, one that arises from a semi-volatile source (presumably from 2-methyl tetrols directly evaporating) and one that arises from the thermal decomposition of a low volatility source and a desorption signal that corresponds to $C_5H_{10}O_3$, which also arises from the thermal decomposition of a low volatility source. Because knowledge of the molecular composition of IEPOX-SOA is critical to the development of accurate SOA mechanistic models, this work will be of great interest to readers of Atmospheric Chemistry and Physics. However, I believe that a number of uncertainties remain in the interpretation of both the present work and past studies, and that a revised manuscript should more directly address these issues.

Specific comments

Because of a lack of authentic standards, there continues to be no proof whatsoever that either the GC/MS signals previously attributed to C5-alkene triols or the present CIMS signals attributed to C5-alkene triols actually correspond to these species. Indeed, Watanabe et al. 2018 showed that these species are among the least thermodynamically favored among a variety of possible $C_5H_{10}O_3$ isomers. I suggest that the manuscript be revised to simply refer to a $C_5H_{10}O_3$ thermal decomposition product and refrain from associating this product with any particular molecular form.

This is a good point. We have changed and clarified wording, specifically on lines 123-125, 294, and 511, however we do think it useful in various places to connect this component to tracers of IEPOX SOA reported in the literature with the same elemental composition.

Similarly, while I find the argument fairly convincing that the semi-volatile $C_5H_{12}O_4$ component is probably the 2-methyl tetrols themselves, I don't think the low volatility thermal decomposition product can be assumed to be the 2-methyl tetrols.

Agree, our point was supposed to be that there is a semi-volatile component with the composition $C_5H_{12}O_4$, likely the tetrol, but also an additional lower volatility component that decomposes into $C_5H_{12}O_4$ during the thermal desorption as reported in field measurements by Lopez-Hilfiker et al. (2016). We have adjusted the wording on lines 294, and 337-338.

The proposed oligomerization mechanism given in Figure 7 would benefit from more detailed discussion. Rather than a more obvious mechanism directly involving IEPOX, the authors are proposing two types of reactions: 1) acid-catalyzed etherification reactions of organosulfates to form ether-linked oligomers and 2) acid-catalyzed sulfate esterification reactions to form sulfate-linked oligomers. The

authors don't provide any literature precedents for these types of reactions. Therefore, I think the authors should provide a rationale for these somewhat unusual reaction types.

We have clarified that the schematic in Figure 7 is a hypothetical set of net transformations to explain the slower shifts in IEPOX SOA volatility and thermogram shape presented in Figure 6. We think a majority of the IEPOX SOA is low volatility, and agree most is indeed formed promptly through IEPOX aqueous phase chemistry to form the organosulfate, or even polyols. These other hypothetical reactions are to offer an explanation for the slower evolution of IEPOX-derived SOA volatility/composition taking place in the absence of IEPOX during isothermal evaporation experiments and at longer times in the batch mode experiments when prompt SOA formation has slowed or even ceased but the SOA continued to age.

Along the same lines, the overall interpretation would benefit from estimates of the thermal desorption behavior of the proposed oligomer components. Did the authors suggest two isomers of a monosulfate dimer as their major proposed molecular species because C₁₀H₂₂SO₁₀ is expected to have roughly the observed thermal desorption behavior?

As stated above, we are unfortunately not able to measure these oligomer (or monomer organosulfate) species as we suspect they are decomposing completely during our analysis. In our response to Yee et al., the final comment, we have estimated c* based on the EVAPORATION group contribution method (Compernelle et al., 2011) for some of these hypothetical structures and find that they are exceedingly low and thus subject to thermal decomposition during the desorption process before evaporation rates would be sufficient to desorb them from the filter in detectable amounts. We refer the reviewer to other work by the Surratt group proposing and observing the presence of polyol esters (Lin et al., 2014; Zhang et al., 2011; Surratt et al., 2006).

Technical comments

Line 87: There should be a reference to Hu et al. 2016 ACP 16, 11563-11580 here.

Reference added.

Line 128: There is something wrong with the grammar in this sentence. Please revise.

We changed the sentence to:

The data presented herein were taken at the Pacific Northwest National Laboratory (PNNL) as part of the Secondary Organic Aerosol Formation from Forest Emissions Experiments (SOAFFEE) campaign held during the summer of 2015.

Line 464: I'm not sure why there is a reference to Atkinson, 1987 here. There are two measurements of IEPOX + OH rate constants: Bates et al. 2014 and Jacobs et al. 2013, ES&T 47, 12868-12876, which differ by a factor of two. The choice of rate constant should be explicitly discussed.

Thank you for pointing this out. The model is very simple so we use one gas-phase OH reaction rate which applies to both the IEPOX and 2-methyltetrol. We used the Atkinson SAR method to determine the OH reaction rate with both 2-methyltetrol and IEPOX. The rate found by the Atkinson method was within the range of values found by Bates et al. and Jacobs et al. We have added the references for

Bates & Jacobs and reworded the sentence (see below) to describe our rate-selection process more clearly and now also include the rate.

We also include a loss of gas-phase species (2-methyltetrol and IEPOX) due to reaction with OH at $1.8 \times 10^{-11} \text{ cm}^3 \text{ molec}^{-1} \text{ s}^{-1}$ (Atkinson, 1987), consistent with previous studies for the IEPOX + OH rate constant (Bates et al., 2014; Jacobs et al., 2013).

Anonymous Referee #2

Overview:

This study sheds new light on the question of volatility and chemical composition of secondary organic aerosol derived from IEPOX, a ubiquitous biogenic aerosol component. IEPOX is known to react in aqueous aerosol to form commonly observed products such as methyltetrols and organosulfates, and compounds with the molecular formula $C_5H_{10}O_3$ (C_5 alkene triols, methyl-tetrahydrofuran-diols, or both) have also been observed in IEPOX SOA. The total reactivity of IEPOX in the aerosol phase and its uptake are known to be highly dependent on aerosol acidity, sulfate content, organic coating, and other parameters, but a detailed chemical understanding of the composition of the resulting organic aerosol is still lacking. Most observations of ambient IEPOX-derived SOA suggest that the majority of the SOA is of lower volatility than the individual species described above, suggesting a greater presence of oligomers and organosulfates and relatively small contributions from methyltetrols, alkene triols, or MeTHF-diols. This work bridges that apparent gap by showing that observed alkene triols or MeTHF-diols are artifacts formed during the thermal decomposition of lower volatility material, as is a portion of the signal observed at the same mass as methyltetrols, while another portion that likely arises from the methyltetrols themselves is volatile and undergoes evaporation from the particle phase on the timescale of 1 hour.

The authors reach these conclusions by observing the uptake of trans-b-IEPOX onto acidified ammonium bisulfate seed aerosol in a series of controlled chamber experiments. They evaluate the evolution of particle chemical composition and component volatility using a high-resolution time-of-flight I- chemical ionization mass spectrometer outfitted with a filter inlet for gases and aerosols, which enables the separation of isobaric compounds by thermal desorption. Thermograms taken at varying humidities and timepoints during the experiments support the assertion that methyltetrols form quickly via direct hydrolysis following IEPOX uptake, and are then both transformed to lower-volatility species and evaporated into the gas phase, where they can be lost to walls or further photooxidation. The remaining IEPOX-derived SOA is therefore of very low volatility, likely including oligomers of the tetrols and organosulfates. Finally, the authors use a simple box model to illustrate how these results might play out under ambient conditions, and show that models using either aqueous uptake or volatility basis set schemes should be modified to account for the high uptake probability of IEPOX followed by re-volatilization of methyltetrols.

While the description of the experiments performed herein and the conclusions drawn from thermal desorption measurements is straightforward and represents a valuable contribution to our understanding of the volatility and chemical composition of IEPOX derived SOA, the extrapolation to ambient conditions remains tenuous and deserves further attention. Additional comparison to ambient results (e.g. Hu et al 2016) would help convince the reader that the results from these chamber studies are borne out in the atmosphere and are relevant to processes that occur in isoprene- and sulfate rich settings. The brief comparison on lines 221-232 is not sufficient, and if anything brings up more questions than it answers as to the validity of comparing field to laboratory results. Does Lopez-Hilfiker et al. suggest that a further 50% of IEPOX SOA observed in ambient consists of tracers that don't even correlate with those identified here, in addition to the fraction that correlates with them but isn't explicitly $C_5H_{12}O_4$ or $C_5H_{10}O_3$? What are those other tracers and what could explain their absence in these experiments? Ambient particles likely contain much more variability in organic compounds in the

condensed phase with which tetrols and other IEPOX-derived species might oligomerize or otherwise interact. How would that affect the conclusions here and our ability to put simple parameterizations into models? Is there any evidence that products of such cross-reactions result in similar observed compounds upon thermal decomposition?

See the response to comments by Yee et al., opening statement and section II c. To summarize point by point here:

1. We further discuss the ambient measurements on lines 281-289, and now cite Hu et al. 2016 on lines 89-90 and 377.
2. Due to the underestimated contribution from furan diols, the stated 50% explanation of the IEPOX PMF factor mass from the AMS is a conservative underestimate which is discussed within the reference.
3. We agree, with more complexity in the atmosphere it is possible and even likely that other species will oligomerize with IEPOX itself or its reaction products, leading to a more complex picture discussed herein. If these monomeric units oligomerize with different species in the atmosphere, forming different linkages, this will affect their lifetime. The different linkages may also affect the compounds observed upon thermal desorption as noted. However, we measure these monomers in the atmosphere, as have numerous other studies, and rather few other components in our mass spectra correlate with these specific tracers over time, suggesting that the products of a broader set of cross reactions either decompose into the same monomeric composition, are not significant contributors, or are for some reason not strongly correlated with the other IEPOX tracers. However, this complexity does not change the main conclusions of our work or implications for modeling, mainly that IEPOX SOA components with the formula $C_5H_{12}O_4$ likely represent a major prompt product of IEPOX reactive uptake, but are semi-volatile and thus can partition to the gas-phase, and otherwise remaining components detected as $C_5H_{12}O_4$ or $C_5H_{10}O_3$ in the particle phase are likely decomposition of lower volatility oligomers or organosulfates.

Technical comments:

L 136: Is it possible that ethyl acetate interferes at all?

We do not have evidence that it is taken up into the aerosol and would not expect it to as its volatility is very high and solubility rather low. In the continuous flow experiments, the ethyl acetate evaporated completely well before the experiment was over and IEPOX was still present in the chamber. Also, given the similarity between the ambient tracers and chamber SOA composition, it would seem there isn't a major effect.

L 141-143: How does this uncertainty carry through to the conclusions you draw in this study? Since most of your analysis is independent of IEPOX mass, these uncertainties may not affect any major conclusions, but greater discussion of the uncertainties associated with the I- CIMS measurements is warranted. What is the potential for differences in sensitivities to the various compounds measured herein? Is the sensitivity to any given compound known to be constant over the course of a thermogram?

Please see our response to Yee et al. for more detail. Briefly: the I-CIMS is able to measure the species of interest here, namely $C_5H_{10}O_3$ and $C_5H_{12}O_4$, regardless of structure (Iyer et al., 2016). However, whether the $C_5H_{10}O_3$ is an alkene triol or furan diol will affect the sensitivity and thus estimates of mass concentration. We use calibrations to authentic triols and diols to constrain these estimates, and generally use instrument response to C_5 triols which is higher per ng than it is for the diols so that our mass concentration estimates are lower limits. Calibration uncertainties are typically 30-50% based on repeated tests, and usually systematic in nature because precision within any individual calibration test is high. We primarily focus on qualitative behavior or intrinsic relative behaviors (e.g. T_{max}) in this paper, and thus relative sensitivities do not affect our conclusions.

L 144: What were the concentrations of ammonium bisulfate and sulfuric acid, and what size particles did their atomization generate?

We have added this information in lines 148-157, and copied below.

Wet, polydisperse acidic ammonium sulfate seed was generated by atomizing an ammonium bisulfate solution acidified with additional H_2SO_4 . The solution was made by mixing ammonium sulfate (0.1308 g) with sulfuric acid (8.02 mL of 0.2465 M) and diluting to a total volume of 1 L with ultrapure water. The average molar $NH_4^+ : SO_4^{2-}$ ratio measured by the AMS was approximately 0.93 for all experiments, though due to the experimental procedure some interference from organic sulfate formation may exist. The measured $NH_4^+ : SO_4^{2-}$ ratio is significantly higher than was present in the atomized solution, implying that excess gas-phase ammonia present in the chamber partially neutralized the injected seed. The seed surface area concentrations were approximately 37,600 and 24,000-27,000 cm^{-3} and the volume weighted mode diameters were 106 and 244-254 nm in continuous and batch modes, respectively. Continuous flow experiments were conducted at 50% RH, while the RH of batch mode experiments was either 30% or 50%.

L 211-214: This sentence is confusing and may be missing a verb or clause.

Agreed, “when” was changed to “with”.

L 216: Speaking of vapor wall losses, how might the wall loss of the re-evaporated 2-methyltetrols affect the results of this study? If you have a large sink to the walls, might Henry’s law equilibrium effectively pull more tetrol out of the particles that would otherwise occur?

Indeed, this effect of vapor wall loss is quite possible. Operating in continuous flow mode helps achieve a steady state that mitigates effects of reversible vapor wall loss somewhat. In the batch mode experiments, we do not see a significant loss of the low- T_{max} /semi-volatile mode over the experimental time scale. That said, attempts to quantify the IEPOX SOA yield, which was not a goal of this study, do need to consider vapor wall loss of the semi-volatile product. We have added this issue to the implications section when we discuss the evolution of IEPOX SOA and the associated simple box-model (lines 481-490), and copied below.

It is not clear how much vapor wall loss affects the results of this study or if we are underestimating or overestimating IEPOX SOA in the chamber. In the atmosphere, photochemical losses of the semi-volatile tetrol in the gas-phase due to reaction with OH (not present in the chamber) would shift more tetrol out of the particle phase than in our chamber experiments (no OH). Moreover, the much smaller aqueous

volume of ambient aerosol particles in the atmosphere compared to that in the chamber would also lead to more of the tetrol re-partitioning to the gas phase than in the chamber. Thus, while vapor wall loss in the chamber likely lowers particle phase tetrol, that effect might be partially or entirely offset by other processes/conditions which enhance particle phase tetrol in the chamber compared to the atmosphere.

Vapor wall loss is not considered in the model, which might be resulting in more tetrol evaporating from the particles in our measurements than would occur in the atmosphere. However, operating in continuous flow mode helps to mitigate these issues, and in batch mode we do not observe a significant loss of the low- T_{max} /semi-volatile mode. In the atmosphere, photochemical losses of the tetrol and the smaller aqueous volume of the aerosol would lead to partitioning of the tetrol out of the aerosol. Thus, while vapor wall loss in the chamber likely leads to lower particle-phase tetrol, the effect would be offset by these processes in the atmosphere, and so not considering vapor wall loss in the model should not significantly affect our results.

Figure 4: Should there be units on UHP N2?

No, it is simply indicating when there was and was not flow (i.e. on or off). We added an explanation for this to line 307 and the figure caption.

L 335: Is the assumption of no particle-phase diffusion limitations a safe one? How might phase separation or organic coatings change these estimates?

Due to the rapid (1 hour) and nearly complete evaporation of the low T_{max} /high volatility mode of the C₅H₁₂O₄ species, we have no indication that there is a limitation. Thus, while there may well be organic coatings, we can reasonably conclude there is not a sufficient diffusion limitation to evaporation. The observed evaporation rates are consistent with the expected saturation vapor concentration or solubility calculated or inferred from independent methods.

L 339-342: How close do you expect these estimates of the Henry's law constant to be? A variation of two orders of magnitude seems strikingly large.

The quoted range reflects the range of possible values based on the input uncertainties. The COSMOtherm computation estimates are $4.9 \times 10^8 - 1.1 \times 10^{10}$ M atm⁻¹ while the value derived from the observed evaporation rate is more constrained to be $1-2 \times 10^8$ M atm⁻¹. As for saturation vapor concentration estimates, we would treat these quantities as order-of-magnitude estimates given the challenges associated with deriving them both computationally and experimentally in the extremes (low vapor pressures or very high solubilities), and for multifunctional compounds where predictions are especially uncertain (D'Ambro et al., 2017). In the end, $>1 \times 10^8$ M atm⁻¹ is probably sufficient for atmospheric modeling.

L 460: Since other reported values (e.g. Figure 8) are in ug/m³, it would be helpful to report the same units for the starting IEPOX concentration

We added the value in ug/m³ after the value in ppb.

L 460-461: Why were 90% and 10% chosen? How certain are these branchings, and how wide a range might they span in ambient conditions? How sensitive are the simulation results to changes in these numbers, and in the other parameters used?

We have made an educated guess based on previous measurements to the branching ratio, and previous measurements of the IEPOX SOA yield, and thus they are not all that certain. Rather, we use the model as stated, for a simple conceptualization of how $C_5H_{12}O_4$ would behave in the atmosphere. It's quite possible that this branching is correct, but may span to 50/50, but likely not much higher than 50% OS production based on previous work. The simulation should not be overly sensitive to the branching ratio as the aerosol concentration quickly converges to being dominated by the OS due to the semi-volatile nature of the tetrol product at a rate mainly determined by the solubility or saturation vapor concentration of the tetrol and its gas-phase loss rates.

L 463-464: What rates are used for the gas-phase reactions with OH?

We have added the rate, $1.8 \times 10^{-11} \text{ cm}^3 \text{ molec}^{-1} \text{ s}^{-1}$, to the manuscript on line 472.

L 499: Hyphen in the wrong place on "2 methyl-tetrol"?

Yes, fixed now.

Reference:

Hu, W., Palm, B. B., Day, D. A., Campuzano-Jost, P., Krechmer, J. E., Peng, Z., de Sá, S. S., Martin, S. T., Alexander, M. L., Baumann, K., Hacker, L., Kiendler-Scharr, A., Koss, A. R., de Gouw, J. A., Goldstein, A. H., Seco, R., Sjostedt, S. J., Park, J.-H., Guenther, A. B., Kim, S., Canonaco, F., Prévôt, A. S. H., Brune, W. H., and Jimenez, J. L.: Volatility and lifetime against OH heterogeneous reaction of ambient isopreneepoxydiols-derived secondary organic aerosol (IEPOX-SOA), *Atmos. Chem. Phys.*, 16, 11563-11580, <https://doi.org/10.5194/acp-16-11563-2016>, 2016.

Lopez-Hilfiker, F. D., Mohr, C., D'Ambro, E. L., Lutz, A., Riedel, T. P., Gaston, C. J., C4 Iyer, S., Zhang, Z., Gold, A., Surratt, J. D., Lee, B. H., Kurten, T., Hu, W. W., Jimenez, J., Hallquist, M., and Thornton, J. A.: Molecular composition and volatility of organic aerosol in the southeastern US: Implications for IEPOX derived SOA, *Environ. Sci. Technol.*, 50, 2200-2209, doi: 10.1021/acs.est.5b04769, 2016.

References

- Atkinson, R.: A Structure-Activity Relationship for the Estimation of Rate Constants for the Gas-Phase Reactions of OH Radicals with Organic-Compounds *Int. J. Chem. Kinet.*, **19**, 799-828, 10.1002/kin.550190903, 1987.
- Bates, K. H., Crouse, J. D., St Clair, J. M., Bennett, N. B., Nguyen, T. B., Seinfeld, J. H., Stoltz, B. M., and Wennberg, P. O.: Gas phase production and loss of isoprene epoxydiols, *J. Phys. Chem. A*, **118**, 1237-1246, 10.1021/jp4107958, 2014.
- Compernelle, S., Ceulemans, K., and Muller, J. F.: EVAPORATION: a new vapour pressure estimation method for organic molecules including non-additivity and intramolecular interactions, *Atmos. Chem. Phys.*, **11**, 9431-9450, 10.5194/acp-11-9431-2011, 2011.
- D'Ambro, E. L., Lee, B. H., Liu, J., Shilling, J. E., Gaston, C. J., Lopez-Hilfiker, F. D., Schobesberger, S., Zaveri, R. A., Mohr, C., Lutz, A., Zhang, Z., Gold, A., Surratt, J. D., Rivera-Rios, J. C., Keutsch, F. N., and Thornton, J. A.: Molecular composition and volatility of isoprene photochemical oxidation secondary organic aerosol under low- and high-NO_x conditions, *Atmos. Chem. Phys.*, **17**, 159-174, 10.5194/acp-17-159-2017, 2017.
- Iyer, S., Lopez-Hilfiker, F., Lee, B. H., Thornton, J. A., and Kurten, T.: Modeling the Detection of Organic and Inorganic Compounds Using Iodide-Based Chemical Ionization, *Journal of Physical Chemistry A*, **120**, 576-587, 10.1021/acs.jpca.5b09837, 2016.
- Jacobs, M. I., Darer, A. I., and Elrod, M. J.: Rate Constants and Products of the OH Reaction with Isoprene-Derived Epoxides, *Environmental Science & Technology*, **47**, 12868-12876, 10.1021/es403340g, 2013.
- Lin, Y. H., Budisulistiorini, H., Chu, K., Siejack, R. A., Zhang, H. F., Riva, M., Zhang, Z. F., Gold, A., Kautzman, K. E., and Surratt, J. D.: Light-absorbing oligomer formation in secondary organic aerosol from reactive uptake of isoprene epoxydiols, *Environ. Sci. Technol.*, **48**, 12012-12021, 10.1021/es503142b, 2014.
- Lopez-Hilfiker, F. D., Mohr, C., D'Ambro, E. L., Lutz, A., Riedel, T. P., Gaston, C. J., Iyer, S., Zhang, Z., Gold, A., Surratt, J. D., Lee, B. H., Kurten, T., Hu, W. W., Jimenez, J., Hallquist, M., and Thornton, J. A.: Molecular composition and volatility of organic aerosol in the southeastern US: Implications for IEPOX derived SOA, *Environ. Sci. Technol.*, **50**, 2200-2209, 10.1021/acs.est.5b04769, 2016.
- Surratt, J. D., Murphy, S. M., Kroll, J. H., Ng, N. L., Hildebrandt, L., Sorooshian, A., Szmigielski, R., Vermeylen, R., Maenhaut, W., Claeys, M., Flagan, R. C., and Seinfeld, J. H.: Chemical composition of secondary organic aerosol formed from the photooxidation of isoprene, *Journal of Physical Chemistry A*, **110**, 9665-9690, 10.1021/jp061734m, 2006.
- Zhang, H., Surratt, J. D., Lin, Y. H., Bapat, J., and Kamens, R. M.: Effect of relative humidity on SOA formation from isoprene/NO photooxidation: enhancement of 2-methylglyceric acid and its corresponding oligoesters under dry conditions, *Atmos. Chem. Phys.*, **11**, 6411-6424, 10.5194/acp-11-6411-2011, 2011.

Comments prepared by Lindsay Yee, Gabriel Isaacman-VanWertz, and Allen Goldstein

We thank the commenters for their careful reading of our manuscript and helpful comments. Our point-by-point responses are below the comments, highlighted in blue.

Most of the comments by Dr. Yee et al. are centered around how the FIGAERO-CIMS measurements described in our manuscript relate to specific chemical compounds reported by other measurement techniques (e.g. GC/MS), especially given that the FIGAERO-CIMS does not separate by structure/isomer. We think it is therefore helpful to start by summarizing some aspects of FIGAERO-CIMS as a top-down constraint on molecular components and how those inform our main scientific conclusions in this study.

Our goal in this study is not to explain the measurement of specific compounds, such as C₅-alkene triols reported by other instruments, but rather to draw conclusions about the presence of C₅-alkene triols and related isomers generally in ambient SOA and specifically in SOA generated from reactive uptake of IEPOX. We have clarified that our work in no way comments on the potential for C₅-alkene triols to be present in the gas-phase, nor that other measurement techniques may measure C₅-alkene triols from sources other than IEPOX SOA. However, as we discuss below, if C₅-alkene triols and related isomers are in SOA, then the FIGAERO-CIMS would measure them, and this constraint provides insight into the nature of C₅-alkene triols, C₅-furan diols, and related isomers in ambient SOA and IEPOX-derived SOA specifically.

We do not have any reason to expect that the FIGAERO-CIMS using Iodide adduct ionization is not sensitive to C₅-alkene triols, and furan diols, based on direct calibrations of compounds with nearly identical structures shown in part in this manuscript and others (Iyer et al., 2016; Lopez-Hilfiker et al., 2016). Thus, we fully expect to measure C₅-alkene triols and furan diols (Iyer et al., 2016) should they exist in the particle phase. While FIGAERO-CIMS does not speciate across isomers, the signal at C₅H₁₀O₃ is a top-down constraint on the sum-total of C₅-alkene triols, furan diols, hydroxy hydroperoxides, dihydroxy epoxides, hydroxy carboxylic acids, and dihydroxy carbonyls.

Importantly, we have yet to find a structure with the C₅H₁₀O₃ composition that is not detected by FIGAERO-CIMS. We have calibrated to IEPOX, ISOPOOH, alkane triols, and a furan diol with this specific composition, as well as similar hydroxy acids and hydroxy carbonyls (Lee et al., 2014). Thus, the behavior of C₅H₁₀O₃ components in the FIGAERO-CIMS is a constraint on the behavior of commonly measured IEPOX SOA tracers. We think it useful to make this point in the manuscript, that commonly measured tracers of IEPOX SOA reported by other techniques, such as the C₅-alkene triols and furan diols, would fall into this category and be measured by FIGAERO-CIMS.

Summarizing the above, if C₅-alkene triols, furan diols, IEPOX, or ISOPOOH are present in the aerosol, the C₅H₁₀O₃ signal in the FIGAERO-CIMS accounts for that carbon. We likely underestimate the amount of furan diols due to a slightly higher sensitivity to triols, on which we base our conversion of C₅H₁₀O₃ signal to mass concentrations and is a reason we have a low-bias compared to the AMS. That is, stating that the FIGAERO-CIMS accounts for ~50% of IEPOX PMF factor mass from the AMS is a conservative estimate because we currently underestimate contributions from furan diols. It is also possible that the AMS factor is not completely specific to IEPOX derived SOA.

Given that i) we do not observe multiple or broad desorption profiles of C₅H₁₀O₃ (which would possibly imply multiple isomers), ii) that we replicate the field measured desorption profile of C₅H₁₀O₃ in the laboratory using only IEPOX reactive uptake, and iii) that the C₅H₁₀O₃ desorption profile is only consistent with a species having much lower volatility than that of a freely partitioning C₅-alkene triol or furan diol (or IEPOX, ISOPOOH, etc), we conclude that such isomers do not exist in organic aerosol

freely and are instead artifacts of thermal decomposition of a much lower volatility product such as organosulfates, or associated IEPOX-derived oligomers, known independently to also form from IEPOX reactive uptake.

If such components of IEPOX SOA thermally decompose in the FIGAERO, a reasonable hypothesis is that they thermally decompose in other analytical methods that also similarly heat the sample, potentially leading to the same detected tracers ($C_5H_{10}O_3$ isomers). We have reframed our conclusions to make clear that this extrapolation to other methods is a hypothesis that can be tested, and that to some degree has been, and is supported by independent experiments by Cui et al. (2018). More direct comparisons could certainly provide better tests of specific isomers desorbing from IEPOX SOA or other types of organic in different analytical methods.

In light of the uncertainty surrounding the molecular structure(s) that actually lead to observations of C5-alkene triols in chromatography based techniques and $C_5H_{10}O_3$ measurements in CIMS, we think that there are areas of your manuscript that should be adjusted per below:

I. Citation of literature:

- a. Line 87: Reference to Isaacman-VanWertz et al., ES&T 2016 would be appropriate here

Reference added.

- b. Section starting line 289: Why not also compare results to field measurements of volatility as in Hu et al, ACP, 2016, DOI: 10.5194/acp-16-11563-2016?

We have added a reference to Hu et al. (2016) on line 377 when discussing the volatility of the ambient aerosol.

- c. Consider providing additional chemical understanding of proposed compounds in Figure 7 and their expected behavior under programmed thermal desorption and hydrolysis affecting oligomer/accretion products recovery as in Clafin and Ziemann et al., AS&T, 2019, DOI: 10.1080/02786826.2019.1576853. Are your isothermal evaporation results with humidified air providing opportunity for hydrolysis? While lines 52-56 state that your methods confirm that these products are artifacts of thermal decomposition/hydrolysis, hydrolysis is not discussed explicitly elsewhere in the manuscript as it applies to your measurements.

For Figure 7, we are highlighting possible pathways that could explain the time-evolution of our measurements (Figure 6), and effective volatility of IEPOX SOA components that we measured. We have added a statement to this effect on lines 430-432 (copied below) and changed the figure caption to highlight that these are hypothetical processes, albeit based on evidence in other publications. As for hydrolysis, we are evaporating the aerosol at the same RH as their formation, i.e. 50% RH, so we do not believe we would be driving more hydrolysis than would be occurring in the chamber. We have removed the statement about hydrolysis from the abstract.

“...illustrated in Figure 7 which shows hypothetical reaction pathways and oligomers that could explain the observed time-evolution of detected products.”

- d. Lines 224-227: Reword to be more accurate. Lopez-Hilfiker et al., 2016, pg. 2204 states that a sum of tracers in CIMS measurement that are highly correlated with $C_5H_{12}O_4$ and $C_5H_{10}O_3$ explain 50% of IEPOX-SOA factor mass, not just $C_5H_{12}O_4$ and $C_5H_{10}O_3$.

Figure 1 in Lopez-Hilfiker et al. (2016) shows that the sum of FIGAERO-CIMS tracers varies from explaining ~50-90% of the AMS IEPOX-PMF factor. Figure S3 shows that $C_5H_{10}O_3 + C_5H_{12}O_4$ make up >80% of the total sum of tracers (which includes 6 additional ions). Thus our wording on lines 227-230 that the FIGAERO-CIMS $C_5H_{10}O_3 + C_5H_{12}O_4$ make up ~50% of IEPOX SOA mass measured by the AMS is accurate with reference to Lopez-Hilfiker et al. (2016). See also above discussion of the IEPOX SOA reported by the FIGAERO-CIMS in Lopez-Hilfiker et al. (2016) being a conservative estimate.

- e. Line 455: Do you mean Lin et al., ES&T 2014, DOI: 10.1021/es503142b, instead of Lin et al., ES&T 2012, or in addition?

We have added a reference to Lin et al., ES&T 2014 in addition.

- II. Be more precise in language throughout the manuscript relating instrument's observation of a chemical formula (which even stated in line 47 that $C_5H_{12}O_4$ is "presumably" 2-methyltetrols) yet in other areas claim unwarranted certainty in the chemical structure of $C_5H_{12}O_4$ and $C_5H_{10}O_3$. This also needs to be adjusted regarding relation to findings under chamber conditions and then related to atmosphere. Language should be adjusted throughout; some examples specifically listed below:

- a. Lines 52-56: "We thus confirm, using controlled laboratory studies, recent analyses of ambient SOA measurements showing that IEPOX SOA is of very low volatility and commonly measured IEPOX SOA tracers, such as methyltetrols and C5-alkene triols, result predominantly from artifacts of measurement techniques associated with thermal decomposition and/or hydrolysis." As it is not verified if the C5-alkene triol structure is what gives $C_5H_{10}O_3$ in CIMS (standards don't exist yet, though semi-reasonable to assume from a chamber experiment), this statement is not supported enough. Further, Surratt's HILIC method (Cui et al., Environ. Sci. Process. Impacts, 2018) which does measure some higher order organosulfates and oligomers still does not account for all C5-alkene triols as stemming from decomposition (<50%), so is it fair to say predominant? Maybe just predominant for chamber conditions tested here?

As discussed above, our measurement of $C_5H_{10}O_3$ would include C5-alkene triols and 3-MeTHF-3,4-diols, as well as other related isomers. We have changed the wording throughout the manuscript to use the measured formula for the tracers and indicate that they are presumably, but not definitively, the 2-methyltetrols and C5-alkene triols or 3-MeTHF-3,4-diols. We can't think of another structure other than the 2-methyltetrols for $C_5H_{12}O_4$ appearing from authentic IEPOX reacting in the dark in the presence of only aqueous acidic aerosol and no oxidants. We'd happily add a reference to other isomers that would have that composition under those conditions should we be made aware of them.

- b. Lines 220-224: The chemical formulae observed by FIGAERO CIMS are consistent with those from actual chemical species observed by other techniques. Line 221 should be adjusted to something more like, "These chemical formulae are consistent with those of chemical species (i.e. 2-methyltetrols and C5-alkene triols, respectively) that have been repeatedly shown to be major components of IEPOX SOA..."

We have changed the wording to now read: "Species with these compositions have been repeatedly shown to be major components of IEPOX SOA".

- c. While lines 270-278 are precisely worded to state that the interpretation of $C_5H_{10}O_3$ as observed in chamber SOA derives primarily from thermal degradation, this does not warrant broad generalization to the atmosphere as in lines 52-56, lines 494-

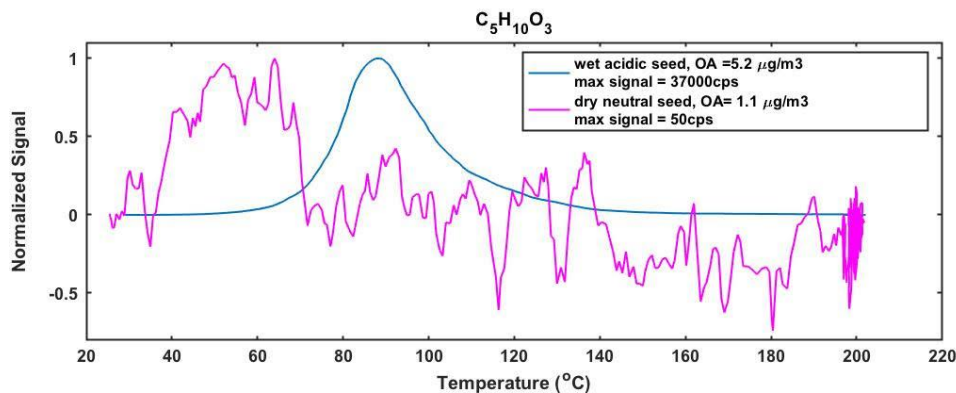
497. Considering there are other potential chemical conditions under which C5-alkene triols may be observed, but not tested here there should be room left for these possibilities, even if less abundant in the atmosphere including:

We basically agree that there are likely multiple sources of C₅H₁₀O₃ during a thermal desorption and this is what we're trying to convey in figure 7. While the isothermal evaporations are evidence that C₅H₁₂O₄ exists partly as a monomer in the particle phase, we don't have any evidence that isomers of C₅H₁₀O₃ from IEPOX uptake exists in a monomer form in the particle phase. Due to the simplicity of the inputs (IEPOX + acidified ammonium sulfate + aqueous seed), there are limited combinations of monomeric units possible in these chamber experiments, hence why two species (C₅H₁₂O₄ & C₅H₁₀O₃) make up such a large portion of our measurements. In addition, the fact that our chamber and ambient thermograms for C₅H₁₀O₃ (Lopez-Hilfiker et al., 2016), figure 1) are rather narrow suggests that what we are measuring also likely comes from compound/s that have similar bond strengths that are breaking within a fairly narrow temperature range to produce C₅H₁₀O₃ (see also Shobesberger et al. (2018)). As noted above, these components have nearly the same effective volatility (T_{max}) as measured by the FIGAERO in chamber generated IEPOX SOA and in ambient OA measured in the field. Thus, the field measurements made with the same instrument and setup (Lopez-Hilfiker et al., 2016), are very similar to the chamber results, and this similarity is the support for concluding more generally about the sources of C₅H₁₀O₃ in IEPOX SOA.

i. IEPOX uptake on non-acidified seed/dry particles:

1. Nguyen et al., ACP, 2014, DOI: 10.5194/acp-14-3497-2014
2. Riva et al., ES&T 2016, DOI: 10.1021/acs.est.5b06050 (Fig. 2 shows C5-alkene triols observed under dry conditions and wet conditions)
3. Lin et al., ES&T 2014, DOI: 10.1021/es503142b (Fig. S2 shows C5-alkene triols observations under wet_neutral and dry_acidic conditions)
4. D'Ambro et al., ACP, 2017, DOI: 10.5194/acp-17-159-2017 (Fig. 4 shows C5H10O3 observation)

We respectfully disagree that the above references represent counter examples to our conclusions. IEPOX can undergo the same ring-opening chemistry and oligomerization in aqueous ammonium sulfate particles which likely have a pH of 4-5 based on aerosol thermodynamic modeling, and will depend on RH (Gaston et al., 2014), only slower. In references 2 and 3, "dry" does not necessarily mean "solid" as the acidification used likely leads to ammonium bisulfate or even sulfuric acid solutions which remain deliquesced even if some ammonium sulfate effloresces at low RH. We show below that the C₅H₁₀O₃ reported in reference 4, which did use effloresced ammonium sulfate seed, is present at nearly 2 orders of magnitude lower mass fraction of the OA with a desorption profile markedly different than the IEPOX tracer discussed in this work.



ii. Non-IEPOX pathways:

1. Liu et al., ES&T 2016, DOI: 10.1021/acs.est.6b01872, as C₅H₁₀O₃ is also observed here reported in Figure 3
2. Riva et al., ES&T 2016, DOI: 10.1021/acs.est.6b02511, as C₅-alkene triols are observed as reported in Figure 1

iii. isoprene ozonolysis leading to structures proposed as sulfate esters of C₅-alkene triols as in Riva et al., Atmos. Env. 2016, DOI: 10.1016/j.atmosenv.2015.06.027)

As noted above, we agree that C₅H₁₀O₃ components could arise from other pathways. But, reference 1 under non-IEPOX pathways is based on the same set of experiments as in reference 4 above, and as noted the C₅H₁₀O₃ in that system behaves nothing like what we describe for the IEPOX system nor what we observe in ambient SOA. As for isoprene ozonolysis leading to sulfate esters, we cannot comment as we have not conducted similar experiments, but our ambient measurements would suggest they either decompose in the FIGAERO the same as IEPOX-derived organosulfates or they are a small contribution to ambient SOA.

III. The connection of FIGAERO-CIMS measurement of C₅H₁₀O₃ being equivalent to the same C₅-alkene triols signal reported from GC-MS is not clear unless an intercomparison was done previously. If done, then please cite the reference:

- a. Lines 494-497: Claim of confirmation that C₅-alkene triols and/or 3-MeTHF-3,4-diols are all artifacts of thermal decomposition is too strong given that it has not been established if what the FIGAERO CIMS measures as these compounds (C₅H₁₀O₃) is actually the same as what other techniques (GC/MS) would assign to be C₅-alkene triols and/or 3-MeTHF-3,4-diols. Where is there direct comparison of FIGAERO-CIMS measured C₅H₁₀O₃ and other techniques measured C₅-alkene triols and/or 3-MeTHF-3,4-diols to prove that the compound/s is/are the same?

We refer to the general discussion above about the top-down constraint provided on these isomers with the FIGAERO CIMS. We have not attempted direct comparisons but agree such could be useful. However, we don't think such comparisons are required to make our conclusions given that the FIGAERO CIMS is sensitive to these isomers, and that using similar or even authentic standards of them demonstrates how different the IEPOX SOA and ambient OA components with the same composition behave during a thermal desorption. For example, we directly compare the thermal desorption of pure 3-MeTHF-3,4-diols to thermal desorptions of the IEPOX SOA components and show they are entirely

inconsistent with these isomers being present as free monomers in the aerosol. Our best explanation is thermal decomposition. The new experiments described here illustrate that another possible explanation, monomers trapped by highly viscous OA, is unlikely due to the rapid and nearly complete evaporation of the species measured at $C_5H_{12}O_4$.

- b. Further, this means the conclusive statement in lines 522-523 is not supported to broadly overgeneralize that GC/MS methods are incorrect. As there are a variety of ways in which GC/MS methods are employed to measure isoprene-derived tracers as well as how the samples are handled and treated before GC/MS analysis, it does not seem appropriate to mention this here without performing proper intercomparisons or going into more specifics as to why all GC/MS methods would lead to thermal decomposition of these products. Thus, statements about specific tracers being "artifacts" or somehow not being useful measurements are misleading and unnecessary. It seems more productive to focus on what the community can learn from the different methods, and what the different tracers teach us, rather than denigrating a particular measurement approach because it sees a combination of products that may include pieces that decompose from larger molecules. For example, the UPLC/HILIC/GC-MS methods provide more specific information (more highly speciated EI mass spectrum of individual tracers that elute from chromatography columns) than the direct CIMS (sum of isomers as a function of desorption temperature) or AMS (EI mass spectrum of the total), but using all the observations we can learn more (not less) about the chemical composition, sources, and transformation processes in organic aerosols.

We stress that our goal is not to denigrate any particular instrument or method. Moreover, we further stress that even though we conclude $C_5H_{10}O_3$ components are detected in the FIGAERO CIMS analysis of IEPOX SOA due to thermal decomposition, those tracers are highly useful for source apportionment of OA. And we agree that the suite of instruments are useful and necessary for making progress on understanding the sources and properties of SOA.

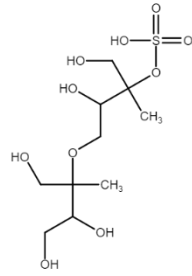
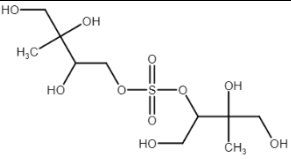
We have made it clearer that our results suggest a hypothesis that other methods that utilize heat in the workup procedures or online analyses would detect IEPOX SOA tracers which are the result of thermal decomposition of low volatility components. We also make it clearer that, using the FIGAERO CIMS specifically, we find no evidence for IEPOX SOA components with an elemental composition of $C_5H_{10}O_3$ and desorption profile consistent with a free monomer partitioning based on its solubility or saturation vapor pressure. The resulting section, which also address points from IIIa above, are on lines 516-523 and below.

We further confirm that the observed properties of $C_5H_{10}O_3$ are not consistent with the structure of C_5 -alkene triols and/or 3-MeTHF-3,4-diols, and thus these structures cannot be components of IEPOX SOA but are likely artifacts of thermal decomposition during analytical workup. A direct intercomparison is required to definitively determine whether all instruments are measuring the same species and that prior estimates of IEPOX SOA have not been overestimated due to "double counting" carbon in these tracers which might be derived from organosulfates and oligomers measured separately.

The evidence presented herein, as well as in independent experiments (Cui et al., 2018), indicates that the $C_5H_{10}O_3$, regardless of structure, as well as a significant portion of the $C_5H_{12}O_4$, are not actual components of the SOA but rather derived from other related components during the analysis. Therefore, we do not recommend that these species be included as products in mechanistic models of IEPOX SOA formation and evolution.

- IV. For some of the structures (organosulfates/polymers) proposed to lead to C₅H₁₀O₃ via decomposition, can you estimate their C*/Tmax and do they make sense with the observed thermograms?

We do not have direct measurements of the species that decompose and lead to the detection of C₅H₁₀O₃ as they do not survive our analysis. However, we can estimate the c* of the dimer species in Figure 7 based on group contribution methods (Compernelle et al., 2011). The very low c* supports the idea that these species with their weaker ether and sulfate bridges will likely undergo decomposition prior to volatilization.

Structure	SMILES	Estimated c* (µg/m ³)
	<chem>CC(CO)(OCC(O)C(C)(CO)OS(O)(=O)=O)C(O)CO</chem>	0.0001
	<chem>CC(O)(CO)C(O)COS(=O)(=O)OC(CO)C(C)(O)CO</chem>	0.00006

References

- Compernelle, S., Ceulemans, K., and Muller, J. F.: EVAPORATION: a new vapour pressure estimation method for organic molecules including non-additivity and intramolecular interactions, *Atmos. Chem. Phys.*, 11, 9431-9450, 10.5194/acp-11-9431-2011, 2011.
- Cui, T., Zeng, Z., dos Santos, E. O., Zhang, Z., Chen, Y., Zhang, Y., Rose, C. A., Budisulistiorini, S. H., Collins, L. B., Bodnar, W. M., de Souza, R. A. F., Martin, S. T., Machado, C. M. D., Turpin, B. J., Gold, A., Ault, A. P., and Surratt, J. D.: Development of a hydrophilic interaction liquid chromatography (HILIC) method for the chemical characterization of water-soluble isoprene epoxydiol (IEPOX)-derived secondary organic aerosol, *Environmental Science: Processes & Impacts*, 10.1039/c8em00308d, 2018.
- Gaston, C. J., Riedel, T. P., Zhang, Z. F., Gold, A., Surratt, J. D., and Thornton, J. A.: Reactive uptake of an isoprene-derived epoxydiol to submicron aerosol particles, *Environ. Sci. Technol.*, 48, 11178-11186, 10.1021/es5034266, 2014.
- Hu, W. W., Palm, B. B., Day, D. A., Campuzano-Jost, P., Krechmer, J. E., Peng, Z., de Sa, S. S., Martin, S. T., Alexander, M. L., Baumann, K., Hacker, L., Kiendler-Scharr, A., Koss, A. R., de Gouw, J. A., Goldstein, A. H., Seco, R., Sjostedt, S. J., Park, J. H., Guenther, A. B., Kim, S., Canonaco, F., Prevot, A. S. H., Brune, W. H., and Jimenez, J. L.: Volatility and lifetime against OH heterogeneous reaction of ambient isoprene-epoxydiols-derived secondary organic aerosol (IEPOX-SOA), *Atmos. Chem. Phys.*, 16, 11563-11580, 10.5194/acp-16-11563-2016, 2016.
- Iyer, S., Lopez-Hilfiker, F., Lee, B. H., Thornton, J. A., and Kurten, T.: Modeling the Detection of Organic and Inorganic Compounds Using Iodide-Based Chemical Ionization, *Journal of Physical Chemistry A*, 120, 576-587, 10.1021/acs.jpca.5b09837, 2016.
- Lee, B. H., Lopez-Hilfiker, F. D., Mohr, C., Kurten, T., Worsnop, D. R., and Thornton, J. A.: An iodide-adduct high-resolution time-of-flight chemical-ionization mass spectrometer: application to atmospheric inorganic and organic compounds, *Environ. Sci. Technol.*, 48, 6309-6317, 10.1021/es500362a, 2014.
- Lopez-Hilfiker, F. D., Mohr, C., D'Ambro, E. L., Lutz, A., Riedel, T. P., Gaston, C. J., Iyer, S., Zhang, Z., Gold, A., Surratt, J. D., Lee, B. H., Kurten, T., Hu, W. W., Jimenez, J., Hallquist, M., and Thornton, J. A.: Molecular composition and volatility of organic aerosol in the southeastern US: Implications for IEPOX derived SOA, *Environ. Sci. Technol.*, 50, 2200-2209, 10.1021/acs.est.5b04769, 2016.
- Schobesberger, S., D'Ambro, E. L., Lopez-Hilfiker, F. D., Mohr, C., and Thornton, J. A.: A model framework to retrieve thermodynamic and kinetic properties of organic aerosol from composition-resolved thermal desorption measurements, *Atmos. Chem. Phys.*, 18, 14757-14785, 10.5194/acp-18-14757-2018, 2018.

1 Chamber-based insights into the factors controlling IEPOX SOA yield,
2 composition, and volatility

3 Emma L. D'Ambro^{1,2}, Siegfried Schobesberger^{1,3}, Cassandra J. Gaston^{1,a}, Felipe D. Lopez-
4 Hilfiker^{1,b}, Ben H. Lee¹, Jiumeng Liu^{4,c}, Alla Zelenyuk⁵, David Bell^{5,d}, Christopher D. Cappa^{6,7},
5 Taylor Helgestad^{6,e}, Ziyue Li⁷, Alex Guenther^{5,f}, Jian Wang^{8,g}, Matthew Wise^{9,h}, Ryan Caylor⁹,
6 Jason D. Surratt¹⁰, Theran Riedel¹⁰, Noora Hyttinen^{11,i}, Vili-Taneli Salo¹¹, Galib Hasan¹¹, Theo
7 Kurtén¹¹, John E. Shilling⁴, Joel A. Thornton^{1,2}

8
9 ¹Department of Atmospheric Sciences, University of Washington, Seattle WA, USA

10 ²Department of Chemistry, University of Washington, Seattle WA, USA

11 ³Department of Applied Physics, University of Eastern Finland, Kuopio, Finland

12 ⁴Atmospheric Sciences and Global Change Division, Pacific Northwest National Laboratory,
13 Richland WA, USA

14 ⁵Environmental Molecular Sciences Laboratory, Pacific Northwest National Laboratory,
15 Richland WA, USA

16 ⁶Department of Civil and Environmental Engineering, University of California, Davis CA, USA

17 ⁷Atmospheric Science Graduate Group, University of California, Davis CA, USA

18 ⁸Environmental and Climate Sciences Department, Brookhaven National Laboratory, Upton NY,
19 USA

20 ⁹Department of Math and Science, Concordia University, Portland OR, USA

21 ¹⁰Department of Environmental Sciences and Engineering, Gillings School of Global and Public
22 Health, University of North Carolina, Chapel Hill NC, USA

23 ¹¹Department of Chemistry and Institute for Atmospheric and Earth System Research (INAR),
24 University of Helsinki, Helsinki, Finland

25 ^anow at: Rosenstiel School of Marine & Atmospheric Science, University of Miami FL, USA

26 ^bnow at: TofWerk AG, Thun, Switzerland

27 ^cnow at: School of Environment, Harbin Institute of Technology, Harbin, Heilongjiang, China

28 ^dnow at: Laboratory of Atmospheric Chemistry, Paul Scherrer Institute, PSI-Villigen,
29 Switzerland

30 ^enow at: California Air Resources Board, Sacramento CA, USA

31 ^fnow at: Department of Earth System Science, University of California, Irvine, USA

32 ^gnow at: Center for Aerosol Science and Engineering, Department of Energy, Environmental and
33 Chemical Engineering, Washington University in St. Louis, St. Louis MO, USA

34 ^hnow at: Department of Chemistry, University of Colorado, Boulder CO, USA

35 ⁱnow at: Nano and Molecular Systems Research Unit, University of Oulu, Oulu, Finland

36
37
38
39
40
41

42 Abstract

43 We present measurements utilizing the Filter Inlet for Gases and Aerosols (FIGAERO)
44 applied to chamber measurements of isoprene-derived epoxydiol (IEPOX) reactive uptake to
45 aqueous acidic particles and associated SOA formation. Similar to recent field observations with
46 the same instrument, we detect two molecular components desorbing from the IEPOX SOA in
47 high abundance: $C_5H_{12}O_4$ and $C_5H_{10}O_3$. The thermal desorption signal of the former, presumably
48 2-methyltetrols, exhibits two distinct maxima, suggesting it arises from at least two different
49 SOA components with significantly different effective volatilities. Isothermal evaporation
50 experiments illustrate that the most abundant component giving rise to $C_5H_{12}O_4$ is semi-volatile,
51 undergoing nearly complete evaporation within 1 hour, while the second, less volatile,
52 component remains unperturbed and even increases in abundance. We thus confirm, using
53 controlled laboratory studies, recent analyses of ambient SOA measurements showing that
54 IEPOX SOA is of very low volatility and commonly measured IEPOX SOA tracers such as
55 $C_5H_{12}O_4$ and $C_5H_{10}O_3$, presumably 2-methyltetrols and C_5 -alkene triols or 3-MeTHF-3,4-diols,
56 result predominantly from thermal decomposition in measurement techniques using thermal
57 desorption or prolonged heating for analysis of SOA components. We further show that IEPOX
58 SOA volatility continues to evolve via acidity enhanced accretion chemistry on the timescale of
59 hours, potentially involving both 2-methyltetrols and organosulfates.

60

61 Introduction

62 Aerosols less than 1 μm in diameter play particularly important roles in the Earth's
63 radiative balance and air quality, a large fraction of which is organic carbonaceous material of
64 biogenic origin (~70%) (Hallquist et al., 2009). Isoprene, with a global emission rate of 500 TgC
65 year⁻¹ (Guenther et al., 2012), has the potential to form significant quantities of secondary
66 organic aerosol (SOA). The ability of a volatile organic compound (VOC) to form SOA depends
67 on either of two factors: the efficiency of its oxidative conversion to lower volatility products
68 that can partition to the condensed phase, or the reaction of gas-phase oxidation products in the
69 condensed phase to form products which remain in the condensed phase. Each of these two SOA
70 formation mechanisms have been heavily studied in the case of isoprene.

71 The atmospheric oxidation of isoprene under low NO conditions typically proceeds by
72 OH radicals, leading to the formation of first generation isoprene hydroxy hydroperoxides
73 (ISOPOOH) in high yield (70%) (Paulot et al., 2009). The remaining double bond of isoprene
74 can then undergo another OH addition, leaving a carbon-centered radical adjacent to a
75 hydroperoxide moiety. This radical can internally rearrange to form an epoxy diol (IEPOX) at a
76 yield of ~70-80% (St Clair et al., 2016) or undergo addition of O_2 to form a peroxy radical. The
77 peroxy radical undergoes bimolecular reactions to form closed shell hydroperoxide or nitrate
78 products, or unimolecular H-shifts to form carbonyl- and epoxide-containing products (Paulot et
79 al., 2009; D'Ambro et al., 2017b). The bimolecular peroxy radical reaction products have been
80 shown to be of sufficiently low volatility to partition to the aerosol-phase (D'Ambro et al., 2017a;
81 Liu et al., 2016), and IEPOX has been shown to react in aqueous acidic particles, forming SOA.
82 Commonly measured species from IEPOX reactive uptake include 2-methyltetrols (Lin et al.,
83 2012; Surratt et al., 2006; Wang et al., 2005; Surratt et al., 2010), C_5 -alkene triols (Lin et al.,
84 2012; Surratt et al., 2010; Surratt et al., 2006; Wang et al., 2005), organosulfates (Lin et al.,
85 2012; Surratt et al., 2010; Surratt et al., 2007b; Surratt et al., 2007a), 3-methyltetrahydrofuran-
86 3,4-diols (3-MeTHF-3,4-diols) (Lin et al., 2012), and oligomers (Lin et al., 2012; Surratt et al.,
87 2010; Lin et al., 2014).

88 Recently, studies have called into question whether these commonly measured
89 monomeric products of IEPOX multiphase chemistry exist in the particle-phase as measured
90 (Isaacman-VanWertz et al., 2016; Hu et al., 2016). We showed previously that components of
91 organic aerosol in the Southeast U.S. with compositions of $C_5H_{10}O_3$ and $C_5H_{12}O_4$ desorbed at
92 much higher temperatures, and therefore much lower volatilities, than would be expected based
93 on their composition (Lopez-Hilfiker et al., 2016). We concluded that the measured
94 compositions arise from lower volatility material in the SOA that thermally decomposes rather
95 than evaporating as the native species, and that, based on the relative abundance of these lower
96 volatility components, IEPOX SOA as a whole is typically comprised of very low volatility
97 material. When IEPOX was reacted in bulk solutions and analyzed via nuclear magnetic
98 resonance, no evidence was found for the production of C_5 -alkene triols or 3-MeTHF-3,4-diols,
99 and although a second isomer of the MeTHF diol was observed (3-MeTHF-2,4-diols), the
100 formation rate from IEPOX was calculated to be so slow relative to nucleophilic addition that its
101 formation would be limited to situations where the aerosol had low water content (Watanabe et
102 al., 2018). These findings were further corroborated by comparing a novel chromatography
103 technique that does not involve heating to traditional GC/EI-MS analysis of IEPOX SOA
104 compositions, finding that alkene triols and 3-MeTHF-3,4-diols were in fact formed via thermal
105 decomposition of 2-methyltetrol sulfates and 3-methyltetrol sulfates, respectively (Cui et al.,
106 2018).

107 An additional challenge to understanding IEPOX SOA is that there remains a large gap in
108 carbon closure resulting from IEPOX reactive uptake to aqueous acidic aerosol particles.
109 Although the reactivity of IEPOX in acidic particles is high (Gaston et al., 2014), the SOA yield
110 per reactive loss of IEPOX to particles is relatively low and varies greatly depending on aerosol
111 composition, from approximately 3 to 21% (Riedel et al., 2015). This disconnect may present an
112 inconsistency in models that simulate both IEPOX and IEPOX-derived SOA. If such low yields
113 are indeed realistic, models that adjust the rate of IEPOX reactive uptake to match the IEPOX
114 SOA tracer concentrations without accounting for the lower yield may not correctly simulate
115 IEPOX distributions where reactive uptake is a dominant sink for IEPOX (Gaston et al., 2014).

116 In this work we seek to understand the nature of products formed via the reactive uptake
117 of IEPOX in aqueous acidic particles and the flow of carbon between the gas- and particle-
118 phases. We present measurements from the Pacific Northwest National Laboratory (PNNL,
119 Richland WA) environmental chamber during the 2015 SOA Formation from Forest Emissions
120 Experiment (SOAFFEE) campaign. Batch and continuous flow mode experiments were
121 performed with authentic *trans*- β -IEPOX, which is the dominant isomer (Bates et al., 2014), and
122 wet acidic seed to study the products of IEPOX uptake and the resulting aerosol properties. The
123 properties of commonly measured IEPOX uptake products, $C_5H_{12}O_4$ (presumably 2-
124 methyltetrols) and $C_5H_{10}O_3$ (presumably C_5 -alkene triols or 3-MeTHF-3,4-diols), such as
125 volatility and solubility, are examined in the context of experiments utilizing isothermal
126 evaporation of the formed SOA. The effect of acidity versus liquid water content on the products
127 formed is also discussed, along with implications for modeling atmospheric IEPOX and its
128 conversion into SOA.

129

130 **Experimental Methods**

131 The data presented herein were taken at the Pacific Northwest National Laboratory
132 (PNNL) as part of the Secondary Organic Aerosol Formation from Forest Emissions
133 Experiments (SOAFFEE) campaign held during the summer of 2015. PNNL's 10.6 m^3

134 fluorinated ethylene propylene (FEP) environmental chamber has been described in detailed
135 previously (Liu et al., 2012). The chamber was run in both batch mode and continuous flow
136 mode. In batch mode the experiments lasted ~10 hours, while in continuous flow mode the total
137 flow rate was 48.2 L min⁻¹ resulting in a residence time of ~3.7 hours.

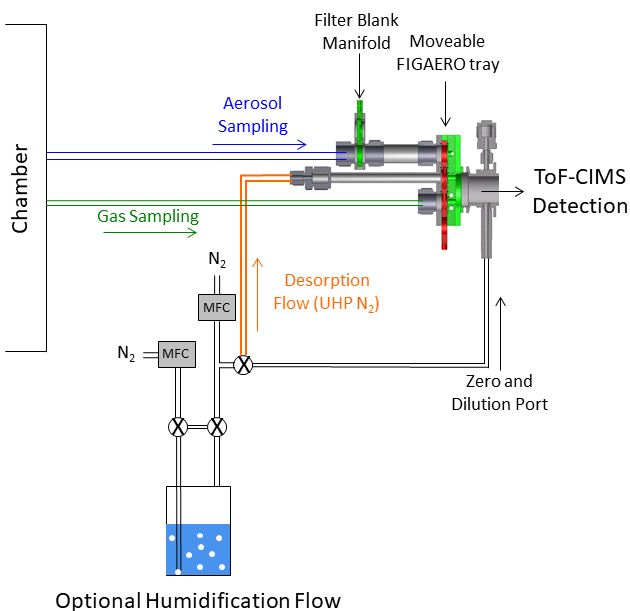
138 Aliquots of an authentic *trans*- β -IEPOX standard which was synthesized according to
139 Zhang et al. (2012) and dissolved in ethyl acetate were injected into a glass bulb which was
140 connected to the chamber via ~10 cm of 1/4" OD polytetrafluoroethylene (PTFE) tubing. Enough
141 IEPOX was added to the empty chamber, before seed addition, to achieve 2 ppb in steady state
142 and at the beginning of batch modes. The bulb and transfer line were heated to 30-40 °C and a
143 100-300 sccm flow of zero air passed over the IEPOX to vaporize and carry it into the chamber.
144 Typically, we measured ~ 10 $\mu\text{g m}^{-3}$ of IEPOX prior to aqueous seed addition. Given calibration
145 uncertainties of ~ +/- 30% from repetitive injections and analytical errors, and potential losses on
146 chamber and sampling surfaces, we estimate an uncertainty of approximately +/- 50% for gas
147 phase IEPOX concentrations and other tracers. Wet, polydisperse acidic ammonium sulfate seed
148 was generated by atomizing an ammonium bisulfate solution acidified with additional H₂SO₄.
149 The solution was made by mixing ammonium sulfate (0.1308 g) with sulfuric acid (8.02 mL of
150 0.2465 M) and diluting to a total volume of 1 L with ultrapure water. The average molar
151 NH₄⁺:SO₄²⁻ ratio measured by the AMS was approximately 0.93 for all experiments, though due
152 to the experimental procedure some interference from organic sulfate formation may exist. The
153 measured NH₄⁺:SO₄²⁻ ratio is significantly higher than was present in the atomized solution,
154 implying that excess gas-phase ammonia present in the chamber partially neutralized the injected
155 seed. The seed surface area concentrations were approximately 37,600 and 24,000-27,000 cm⁻³
156 and the volume weighted mode diameters were 106 and 244-254 nm in continuous and batch
157 modes, respectively. Continuous flow experiments were conducted at 50% RH, while the RH of
158 batch mode experiments was either 30% or 50%.

159 A suite of online gas and particle-phase instrumentation was used to monitor
160 concentrations throughout the experiments. Aerosol number and volume concentrations were
161 measured with a scanning mobility particle sizer (SMPS, TSI model 3936), O₃ and NO/NO₂/NO_x
162 concentrations were monitored with commercial instrumentation (Thermo Environmental
163 Instruments models 49C and 42C, respectively). An Aerodyne high-resolution time-of-flight
164 mass spectrometer (HRTof-AMS) was utilized to measure bulk submicron organic and
165 inorganic aerosol composition.

166 A high-resolution time-of-flight chemical ionization mass spectrometer (HRTof-CIMS)
167 using iodide adduct ionization was deployed for the detection of both semi- and low-volatility
168 organic compounds (Lee et al., 2014). The HRTof-CIMS was used to monitor the evolving
169 concentrations of both the precursor (IEPOX) and reaction products in both the gas- and particle-
170 phases when coupled to a Filter Inlet for Gases and AEROSols (FIGAERO), from here on
171 referred to as FIGAERO-CIMS. The coupling, optimization, and operation of this combination
172 has been described in detail previously (Lopez-Hilfiker et al., 2014) and is nearly identical to
173 previous operations (D'Ambro et al., 2017a; D'Ambro et al., 2017b). Briefly, the FIGAERO is an
174 inlet manifold that allows for semi-continuous measurements of both gases and aerosols with
175 approximately hourly resolution. Aerosol was collected on a 24 mm PTFE filter for 43 minutes
176 at 2.5 L min⁻¹, during which the gases were measured in real time. Following collection,

177 programmatically heated ultra-high purity (UHP) N₂ was passed over the filter, while the
 178 temperature was ramped from ambient to 200 °C at a rate of 10 °C min⁻¹ in order to thermally
 179 desorb compounds from the particle-phase to the gas-phase to be carried into the CIMS for
 180 detection. After the temperature was ramped, it was held at 200 °C for 50 minutes to allow
 181 species to desorb and signals to return to background levels. Particle blanks were conducted
 182 approximately every fourth desorption during continuous flow mode or at the beginning and end
 183 of each batch mode experiment by inserting a secondary filter upstream of the primary
 184 FIGAERO filter in order to get a measure of the gas adsorption artifact on the primary filter. Gas
 185 zeros were conducted every 2 minutes by over blowing the CIMS pinhole flow with UHP N₂.
 186 The specific coupling to a HRToF-CIMS with iodide ions allows detailed molecular analysis of
 187 hundreds of oxygenated organic compounds via a clustering, fragmentation-free ionization
 188 process.

189 The FIGAERO-CIMS was also utilized to perform isothermal evaporation experiments as
 190 have been described previously (D'Ambro et al., 2018). In normal operation, the programmatic
 191 thermal desorption is begun immediately after moving the FIGAERO filter under the heating
 192 tube. During isothermal evaporation experiments however, the aerosol is instead exposed for one
 193 hour to a stream of ambient temperature UHP N₂ humidified to 50% RH by using a water
 194 bubbler and two mass flow controllers (Figure 1). After the hour exposure, the N₂ flow is
 195 reverted to its normal dry state and the programmatic heating proceeds as normal. See Figure 1
 196 for the experimental setup. The RH of 50% during evaporation periods was chosen to match that
 197 of the chamber to keep the phase state of the collected aerosols the same (i.e. so as to not drive
 198 efflorescence). Only the isothermal evaporation portion of the experiment was humidified;
 199 during the thermal desorption the bubbler was isolated using two solenoid valves. Passing excess
 200 humidified N₂ over the aerosol and into the instrument resulted in a constant dilution of the
 201 vapor-phase, which allowed for any semi-volatile material to evaporate and also be carried into
 202 the CIMS for detection.

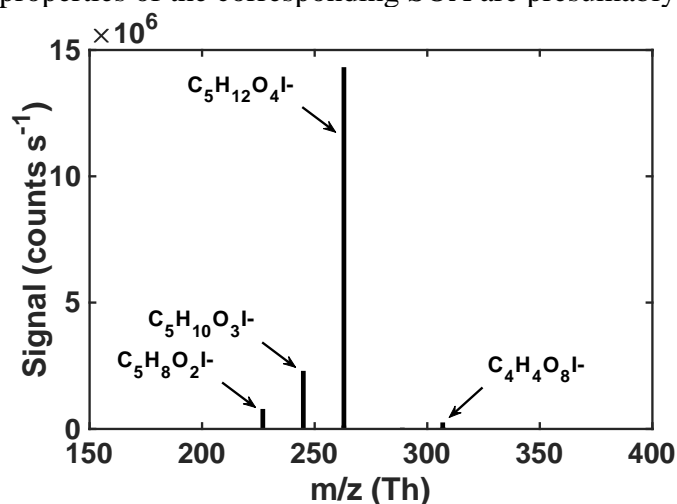


203
 204 **Figure 1.** Schematic of the FIGAERO isothermal evaporation setup.

205
 206 **Results & Discussion**
 207 *Chamber-generated IEPOX SOA Composition and Volatility*

208 Our primary goals with this experiment were to assess whether chamber-generated
209 IEPOX SOA had a composition and volatility similar to that inferred from field measurements
210 using the FIGAERO-CIMS of various IEPOX tracers and to test whether IEPOX SOA as a
211 whole or some of its components were semi-volatile as expected from mechanistic and kinetic
212 considerations. Overall, the estimated mass yield of OA from IEPOX exposure to aqueous acidic
213 seed was generally less than unity, of order 0.5 to less than 0.25, somewhat higher than estimates
214 from Riedel et al [2015]. Mean organic aerosol (OA) mass concentrations generated with IEPOX
215 and aqueous acidic seed were $2.5 \mu\text{g m}^{-3}$ for steady state conditions, $5.5 \mu\text{g m}^{-3}$ at the beginning
216 of the 30% RH batch experiment, and $4.5 \mu\text{g m}^{-3}$ at the beginning of the 50% RH batch
217 experiment. The OA to sulfate ratio was observed to evolve during a batch experiment (e.g.,
218 decreasing by 20% from the peak), and given the uncertainties associated with potential vapor
219 wall losses of IEPOX and its reaction products, we refrain from quantitatively interpreting the
220 SOA yield behaviors in detail.

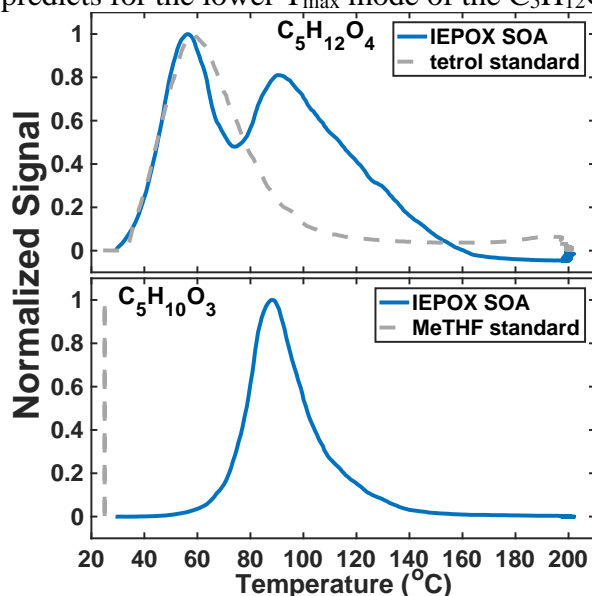
221 Regardless of the conditions, the uptake of an authentic IEPOX standard onto acidic
222 seeds in these experiments results in a rather simple observed particle-phase composition upon
223 thermal desorption. As shown in Figure 2, a few compositions dominate the average particle-
224 phase mass spectra, most predominantly $\text{C}_5\text{H}_{12}\text{O}_4\text{I}^-$ and $\text{C}_5\text{H}_{10}\text{O}_3\text{I}^-$. Species with these compositions
225 have been repeatedly shown to be major components of IEPOX SOA (Lin et al., 2012; Surratt et
226 al., 2010; Surratt et al., 2006; Wang et al., 2005), although the relative abundances could change
227 with time or conditions. In ambient aerosol in the Southeast U.S., the same FIGAERO-CIMS
228 instrument detected $\text{C}_5\text{H}_{12}\text{O}_4$ and $\text{C}_5\text{H}_{10}\text{O}_3$ in SOA, and these tracers correlated with and
229 explained $\sim 50\%$ of the IEPOX SOA mass derived from factor analysis of aerosol mass
230 spectrometer (AMS) data (Lopez-Hilfiker et al., 2016). Our laboratory chamber experiments
231 starting with an authentic IEPOX standard and acidic seed without photochemical oxidants
232 therefore support the use of these FIGAERO-CIMS compositions as tracers of IEPOX SOA in
233 atmospheric particles. As these two compositions are such a large component of the particle-
234 phase signal (97.5%) measured by FIGAERO-CIMS in chamber generated IEPOX SOA, the
235 properties of the corresponding SOA are presumably similar to their properties.



236
237 **Figure 2.** Average mass spectrum of IEPOX-derived SOA at a total OA concentration of $5 \mu\text{g m}^{-3}$.
238

239 In previous work, we have related the temperature at which the ion signal for a given
240 molecular composition reaches a maximum during a desorption, known as the T_{max} , to the
241 enthalpy of vaporization (or sublimation) and thus effective volatility (Lopez-Hilfiker et al.,

242 2014). Effective volatility refers to the fact that the thermal desorption signal is a convolution of
 243 evaporation, thermal decomposition, particle viscosity, and mass transfer of desorbed vapors
 244 through the apparatus, and not solely saturation vapor pressure. Notably, the thermogram of
 245 $C_5H_{12}O_4$ for chamber generated IEPOX SOA is bimodal (Figure 3, top), i.e. it exhibits two
 246 distinct maxima, one occurring at $T_{max} = 55\text{ }^\circ\text{C}$ ($\sim 40\%$ of signal), and a second mode at $T_{max} =$
 247 $90\text{ }^\circ\text{C}$. These two maxima indicate SOA components with orders of magnitude different effective
 248 volatilities contribute to the desorption of $C_5H_{12}O_4$. For example, using the calibration curve in
 249 Lopez-Hilfiker et al. (2014) relating saturation vapor concentration (c^*) to T_{max} , the two modes
 250 correspond to SOA components with an effective c^* of 50 and $0.005\text{ }\mu\text{g m}^{-3}$. The lower
 251 temperature, higher volatility mode of the $C_5H_{12}O_4$ desorption has a T_{max} consistent with that of
 252 an authentic 2-methyltetrol standard, synthesized according to Bondy et al. (2018), deposited on
 253 the filter (gray dashed line, Figure 3, top). For comparison, if the structure of $C_5H_{12}O_4$ were
 254 assumed to be a 2-methyltetrol, group contribution methods predict the c^* to be $34\text{ }\mu\text{g m}^{-3}$
 255 (Compernelle et al., 2011), remarkably similar to what the FIGAERO T_{max} - c^* relationship
 256 predicts for the lower T_{max} mode of the $C_5H_{12}O_4$ thermogram.



257
 258 **Figure 3.** Thermal desorption profiles of chamber aerosol (blue) and calibrations with authentic
 259 standards (gray, dashed) of the two major particle-phase compounds detected in the chamber:
 260 $C_5H_{12}O_4$ (top) and $C_5H_{10}O_3$ (bottom).
 261

262 The $C_5H_{10}O_3$ thermogram, in contrast, is monomodal, suggesting a single component
 263 giving rise to its desorption. However, the T_{max} is much higher than the corresponding authentic
 264 *cis*-3-MeTHF-3,4-diol standard, synthesized according to Zhang et al. (2012), (and also that of
 265 an alkane triol standard). This standard desorbs completely from the FIGAERO filter in seconds
 266 without heating (gray dashed line, Figure 3, bottom). The T_{max} of $C_5H_{10}O_3$ desorbing from
 267 IEPOX SOA is $90\text{ }^\circ\text{C}$, the same as the higher T_{max} mode of the $C_5H_{12}O_4$ component, and thus
 268 implies a SOA component with an effective c^* of at most $0.005\text{ }\mu\text{g m}^{-3}$, indicative of thermal
 269 decomposition during desorption. For comparison, if the structure is assumed to be a C_5 -alkene
 270 triol or 3-MeTHF-3,4-diol, group contribution methods would predict a much larger c^* of ~ 60 or
 271 $1.3 \times 10^5\text{ }\mu\text{g m}^{-3}$, respectively (Compernelle et al., 2011). For comparison, the group contribution
 272 predicted c^* of *trans*- β -IEPOX is $1.7 \times 10^4\text{ }\mu\text{g m}^{-3}$. All of this evidence indicates that $C_5H_{10}O_3$, as
 273 detected in the chamber-generated SOA, is a result of thermal decomposition of a lower

274 volatility species, consistent with recent studies that found the C₅-alkene triol was not present as
275 a product of bulk IEPOX reactions (Watanabe et al., 2018) or when the IEPOX SOA was
276 analyzed with novel methods not involving heating (Cui et al., 2018). Taken together, the
277 thermograms of C₅H₁₂O₄ and C₅H₁₀O₃ therefore indicate a large fraction of the chamber
278 generated IEPOX SOA is composed of very low volatility material (effective c* << 1 μg m⁻³)
279 and several orders of magnitude lower volatility than the compounds that are detected upon
280 thermal desorption.

281 The thermogram behaviors of chamber generated IEPOX SOA are entirely consistent
282 with those observed for the same tracers measured in ambient aerosol in the Southeast U.S.,
283 where C₅H₁₂O₄ was also detected with two modes in the thermogram, the respective areas of
284 which varied relative to each other over the course of the measurement campaign (Lopez-
285 Hilfiker et al., 2016). Lopez-Hilfiker et al. (2016) demonstrated from these field observations
286 that the abundance and variability of the lower T_{max} (semi-volatile) mode was consistent with an
287 organic compound having the measured molecular composition and c* of the 2-methyltetrol
288 undergoing equilibrium gas-particle partitioning, while the higher T_{max} mode and that of the
289 C₅H₁₀O₃ arose from the decomposition of accretion products.

290

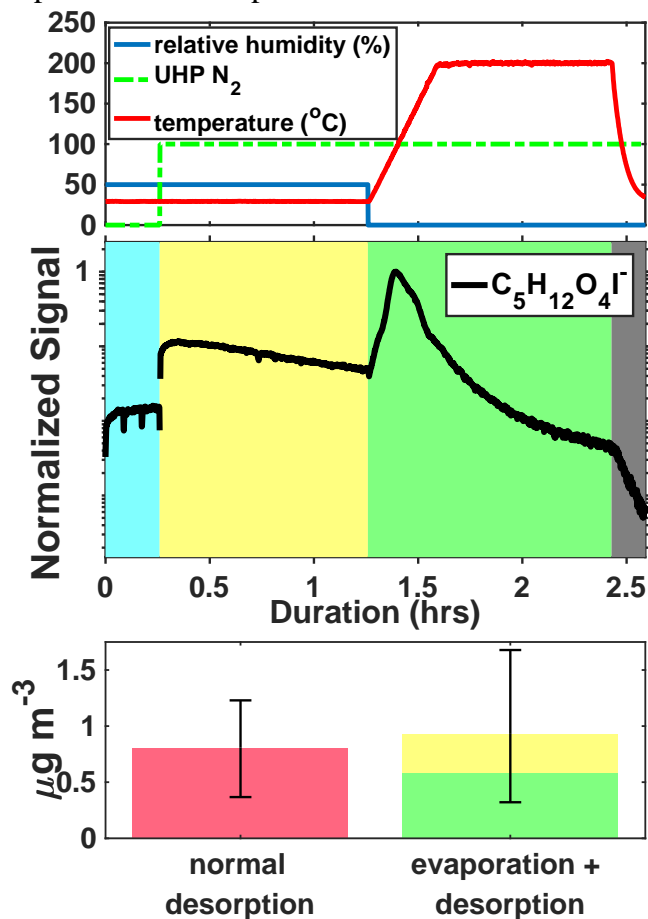
291 *Insights into Volatility via Isothermal Evaporations*

292 The above considerations of chamber generated IEPOX SOA suggest that a large fraction
293 (the high T_{max} mode) should be relatively stable against evaporation upon dilution of the gas-
294 phase, while the lower T_{max} mode of the C₅H₁₂O₄ (likely 2-methyltetrol) component should
295 respond to dilution by evaporating from the particle-phase. To test this hypothesis, we conducted
296 isothermal evaporation experiments using IEPOX SOA generated in the chamber.

297 Figure 4 shows an example ion signal time series during an isothermal evaporation
298 experiment for C₅H₁₂O₄. C₅H₁₂O₄ is detected in the gas-phase during particle collection (middle
299 panel, blue shaded area) when chamber air containing IEPOX, acidic aqueous sulfate particles,
300 and IEPOX SOA was being continuously sampled by the FIGAERO-CIMS. The gas-phase
301 sampling included scanning of the dilution ratio, which resulted in varying signals, as well as
302 periodic zeros resulting in occasional significant short-duration drops in signal. We show the last
303 15-minute portion of the cycle in the gas-phase (blue shaded region) when dilution was held
304 constant, but zeros are still visible as the 2 dips in signal. The chamber was at steady state and
305 the changing gas-phase signal is due to conditioning of the IMR and inlet tubing. During the
306 isothermal evaporation period (yellow shaded area), C₅H₁₂O₄ is also detected when a continuous
307 flow of humidified UHP N₂ (top panel, 100 = desorption flow on) passes over the particles
308 collected from the chamber on the FIGAERO filter and into the mass spectrometer, consistent
309 with C₅H₁₂O₄ evaporation from the collected particles at room temperature (i.e. without heating).
310 Finally, during the temperature-programmed thermal desorption, another pulse of C₅H₁₂O₄ was
311 detected corresponding to components in the remaining SOA that desorbed at elevated
312 temperature (green shaded area).

313 The mass concentration of C₅H₁₂O₄ measured during a normal temperature-programmed
314 thermal desorption is compared to that measured during the isothermal evaporation and
315 subsequent desorption (Figure 4, bottom). Mass closure is achieved to within the experimental
316 error, driven by variance in normal temperature-programmed thermal desorptions due to chamber

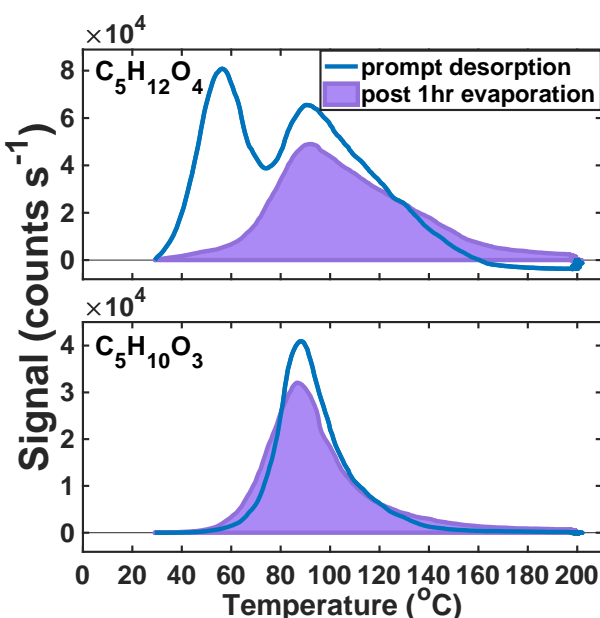
317 conditions and the water vapor effect on CIMS sensitivity (Lee et al., 2014). The observed
 318 behaviors, namely detectable gas-phase concentrations of $C_5H_{12}O_4$ in the chamber and
 319 isothermal evaporation of $C_5H_{12}O_4$ from collected particles indicate that (i) $C_5H_{12}O_4$ is produced
 320 from IEPOX reactive uptake, as expected given that the 2-methyltetrol is predicted to be a major
 321 product (Eddingsaas et al., 2010), and (ii) a portion of the detected $C_5H_{12}O_4$ behaves as a semi-
 322 volatile organic compound (SVOC), being present in both the gas- and particle-phases, and
 323 evaporating promptly from the particle-phase in response to dilution of the surrounding organic
 324 vapors at room temperature.



325
 326 **Figure 4.** Schematic of the isothermal evaporation process. Top: relative humidity (blue), N_2
 327 flow (green, 0 = off, 100 = on), and temperature (red). Middle: $C_5H_{12}O_4I^-$ during a 1-hour
 328 isothermal evaporation experiment shaded by the phase of the experiments: simultaneous real-
 329 time gas-phase sampling and offline aerosol collection (blue), isothermal evaporation where
 330 compounds are measured as they evaporate off the filter (yellow), temperature-programmed
 331 thermal desorption (green), and cool down of the heating tube (gray). Bottom: mass
 332 concentration of $C_5H_{12}O_4$ measured during a normal desorption (pink, left), versus the isothermal
 333 evaporation + desorption (yellow and green, right) for the same chamber conditions.

334
 335 After 1 hour of exposure to UHP N_2 at 50% RH, only 16% of the lower T_{max} mode of the
 336 $C_5H_{12}O_4$ thermogram remains, suggesting near complete evaporation (Figure 5, top). The
 337 observed rate of decay ($84\% \text{ hr}^{-1}$) upon dilution can be related to an effective c^* , or, if the

338 **structure is** 2-methyltetrol it is likely to partition into the aqueous-phase, making an effective
 339 Henry's law constant more appropriate. Assuming no particle-phase diffusion limitations but
 340 accounting for FIGAERO mass transfer limitations (Schobesberger et al., 2018), we predict a c^*
 341 of 5-15 $\mu\text{g m}^{-3}$ for the portion of the $\text{C}_5\text{H}_{12}\text{O}_4$ thermogram that evaporates. Utilizing
 342 COSMOtherm (2018) with the BP_TZVPD_FINE_18 parameterization as described previously
 343 (Kurtén et al., 2018), a Henry's law constant of $4.9 \times 10^8 - 1.1 \times 10^{10} \text{ M atm}^{-1}$ is predicted if all
 344 conformers are used ($4.9 \times 10^8 \text{ M atm}^{-1}$) or if the number of internal H-bonds is minimized
 345 ($1.1 \times 10^{10} \text{ M atm}^{-1}$), which compares well to the value calculated from the observed decay of
 346 $\text{C}_5\text{H}_{12}\text{O}_4$ during the evaporation ($1.8 \times 10^8 \text{ M atm}^{-1}$). These estimates do not include the likelihood
 347 of a salting-out effect expected for 2-methyltetrol (Waxman et al., 2015), which would further
 348 lower the Henry's Law constant. Whether Raoult's or Henry's law is the appropriate framework
 349 for interpretation depends on whether IEPOX reactive uptake results in a phase-separated
 350 organic medium, for example an organic coating, or a homogeneous aqueous solution, and the
 351 competitive partitioning of the $\text{C}_5\text{H}_{12}\text{O}_4$ species between two such regimes. Regardless, as we
 352 show below, the semi-volatile nature of **low T_{max} portion of $\text{C}_5\text{H}_{12}\text{O}_4$, assumed to be the 2-**
 353 **methyltetrol, a major product of IEPOX reactive uptake, will cause it to partition strongly to the**
 354 gas-phase under typical atmospheric conditions outside of cloud.



355
 356 **Figure 5.** Thermograms obtained from prompt desorption of the aerosol (blue) and after
 357 one hour of evaporation (lavender, shaded) of the two major particle-phase compounds detected
 358 in the chamber: $\text{C}_5\text{H}_{12}\text{O}_4$ (top) and $\text{C}_5\text{H}_{10}\text{O}_3$ (bottom).

359
 360 The second, higher T_{max} mode of the $\text{C}_5\text{H}_{12}\text{O}_4$ thermogram and the single Gaussian-like
 361 thermogram of $\text{C}_5\text{H}_{10}\text{O}_3$ (Figure 5, bottom) do not change significantly after 1-hour of exposure
 362 to UHP N_2 . In the case of the $\text{C}_5\text{H}_{10}\text{O}_3$ thermogram, nearly 95% of signal remains after the 1-
 363 hour evaporation period. In both cases, there is a slight broadening of the thermogram and a
 364 measurable increase in material desorbing at the highest temperatures (120+ °C). Previous

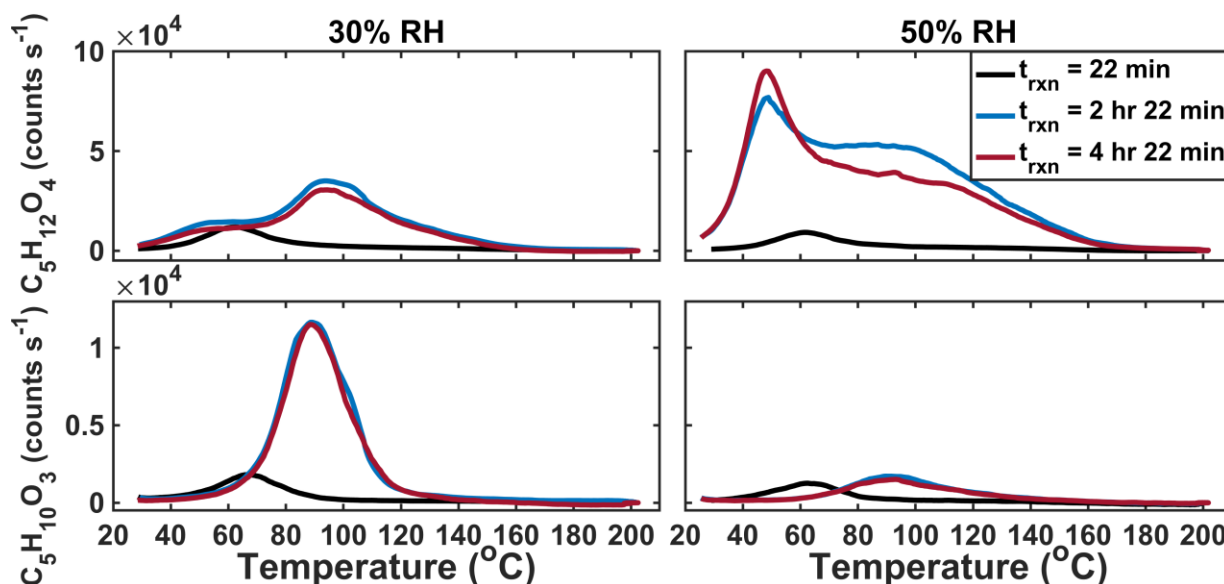
365 isothermal evaporation experiments with the FIGAERO have shown that, for α -pinene
366 ozonolysis SOA, the physical age of the aerosol had a controlling role in the volatility of the bulk
367 SOA and individual desorbing compounds (D'Ambro et al., 2018), consistent with the additional
368 hour of non-oxidative aging in this system resulting in an increase in lower-volatility material.
369 As to the widening of the thermograms, Schobesberger et al. (2018) showed that a shallowing of
370 the low temperature side of the thermogram and a broadening of the higher temperature tail
371 correspond to thermal decomposition from a larger suite of bonds with different dissociation
372 energies, consistent with continued formation of a variety of accretion products during the
373 isothermal evaporation period.

374 The above evidence supports the previous assertions of Lopez-Hilfiker et al. (2016) that
375 the lower T_{\max} mode of the $C_5H_{12}O_4$ thermogram corresponds to a semi-volatile component, very
376 likely the 2-methyltetrol, and further support the conclusion that IEPOX SOA in ambient aerosol
377 is very to extremely low volatility (Lopez-Hilfiker et al., 2016; Hu et al., 2016). The isothermal
378 evaporation experiments presented above provide an explanation as to why the ambient SOA
379 contained such a relatively small fraction of the low T_{\max} (semi-volatile) 2-methyltetrol
380 component in that it likely had evaporated to maintain gas-particle equilibrium. Furthermore, the
381 high T_{\max} tracers do not decay in abundance during the evaporation experiments, but rather
382 slightly increase with time at the highest temperatures (>120 °C), indicating ongoing accretion
383 chemistry leading to lower volatility components.

384

385 *Effect of RH and Acidity on IEPOX SOA Characteristics: Mechanistic Insights*

386 We performed two time-dependent “batch mode” chamber experiments using IEPOX and
387 acidic aqueous seed particles, one at 30% and the other at 50% RH. By operating in batch mode
388 as opposed to continuous flow mode, we are able to temporally resolve the formation of SOA.
389 By varying the RH, we simultaneously varied the liquid water content relative to sulfate, and
390 therefore also acidity. Three sequential thermal desorptions of $C_5H_{12}O_4$ obtained over the course
391 of experiments (~ 10 hrs total) at 30% (left) and 50% (right) RH are shown in Figure 6, top. At
392 30% RH, the lower T_{\max} (higher-volatility) mode grows rapidly and is clearly visible in the
393 first desorption (black line). The first desorption occurred after 43 minutes of particle collection,
394 which began immediately after the seed was injected into the chamber and IEPOX uptake was
395 initiated, resulting in collected aerosols having a variety of ages and thus the median age of 22
396 min is assumed. However, this mode then does not grow significantly larger as the experiment
397 progresses. During the 2nd and 3rd desorptions, 2 hrs 22 min and 4 hrs 22 min respectively, after
398 the initial exposure, the higher T_{\max} (lower-volatility) mode is visible and dominates the
399 thermogram.



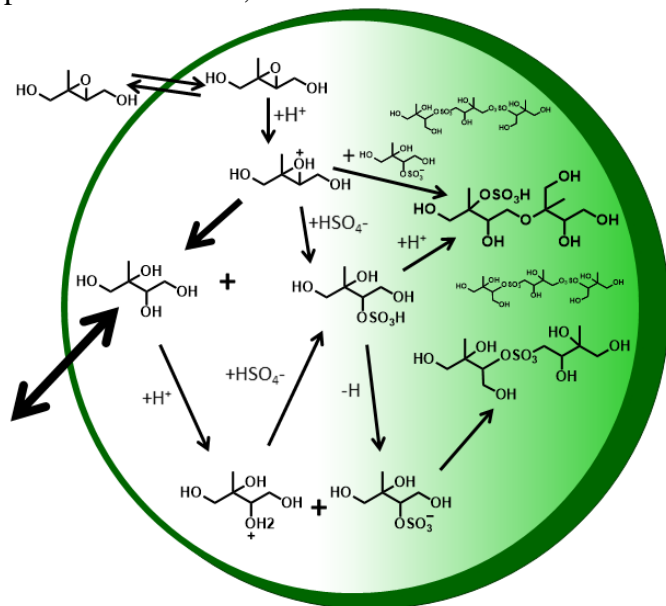
400
 401 **Figure 6.** Sequential desorptions of $C_5H_{12}O_4$ (top) and $C_5H_{10}O_3$ (bottom) during batch mode
 402 experiments at 30% RH (right) and 50% RH (left).

403 In the 50% RH batch experiment, the lower T_{max} (higher-volatility) mode of the $C_5H_{12}O_4$
 404 thermogram also dominates in the first desorption, but in contrast to the experiment at 30% RH,
 405 this lower T_{max} mode continues to grow and is the dominant portion of the thermogram for all
 406 desorptions. While the higher T_{max} mode is observed after the 1st desorption, it is much broader
 407 and has an ambiguous peak, unlike at 30% RH. In the 30% and 50% RH experiments, both
 408 modes of the thermogram are observed by the 2nd desorption 2.5 hours after IEPOX uptake
 409 starts, but the relative abundance and shape of the two modes differ with RH. The thermogram
 410 shape also changes as a function of time since IEPOX injection in the steady state experiments,
 411 although due to the range in aerosol ages present within the chamber at a given time during
 412 steady-state experiments, it is more straightforward to define this feature as a function of time in
 413 batch mode measurements. The corresponding thermograms of $C_5H_{10}O_3$ in each of the two batch
 414 mode experiments are shown in Figure 6, bottom. Most obvious is that the amount of $C_5H_{10}O_3$
 415 desorbing, relative to the $C_5H_{12}O_4$, is highest in the 30% RH experiment, when sulfate and
 416 hydronium ion concentrations are highest. Further work could be done to understand the
 417 evolution of IEPOX SOA components as a function of time, but a fairly stable set of products
 418 and volatility are reached within a few hours.

419 Along with the shape, the T_{max} of the $C_5H_{10}O_3$ and each mode of the $C_5H_{12}O_4$ vary
 420 slightly in time, the two of which are likely related. It has been shown previously that when the
 421 IEPOX-derived organosulfate ($C_5H_{12}SO_7$) is deposited on and desorbed from the FIGAERO
 422 filter, it decomposes into both $C_5H_{12}O_4$ and $C_5H_{10}O_3$. The corresponding T_{max} of both are co-
 423 located and highly dependent on acidity, with higher acidity leading to lower T_{max} 's (Lopez-
 424 Hilfiker et al., 2016). This dependence on the inorganic aerosol components, present in much
 425 larger excess in these experiments than our previous FIGAERO experiments, could be the cause
 426 of the shifts of the lower T_{max} modes. Alternatively, the shift could be due to the increasing
 427 complexity of the SOA as it evolves in time leading to different interactions between particle
 428 components which affects volatility.

429 From these observations we can draw two conclusions regarding the mechanisms that
 430 give rise to the dominant components of IEPOX SOA, illustrated in Figure 7 which shows

431 hypothetical reaction pathways and oligomers that could explain the observed time-evolution of
 432 detected products. First, the low T_{\max} , semi-volatile $C_5H_{12}O_4$ exists in the aerosol from the first
 433 desorption and thus is likely formed promptly from IEPOX uptake, consistent with the formation
 434 of 2-methyltetrol via nucleophilic attack by water of the protonated epoxide ring (see Figure 7).
 435 That this semi-volatile mode is more prominent in the higher RH experiment, i.e. higher liquid
 436 water content and therefore higher H_2O -nucleophile content relative to sulfate, further supports
 437 this interpretation. Additionally, the higher liquid water content supports a greater amount of 2-
 438 methyltetrol remaining partitioned in the aerosol via Henry's Law, consistent with offline filter
 439 analysis (Riva et al., 2016). Second, the higher T_{\max} (lower volatility) modes are mostly
 440 produced more slowly over time, indicating a second or higher generation product of IEPOX
 441 uptake, as these modes are mainly observed 2.5 hours after IEPOX uptake has largely ended.
 442 Thus, if the higher T_{\max} modes are from the thermal decomposition of an organosulfate product,
 443 as suggested by Lopez-Hilfiker et al. (2016) and as Cui et al. (2018) demonstrate, our
 444 experiments suggest it is unlikely to form solely from nucleophilic addition of (bi-)sulfate to
 445 protonated IEPOX, as that reaction should occur concurrently with 2-methyltetrol formation.



446 **Figure 7.** Hypothetical schematic of IEPOX reactive uptake and particle-phase processes. White
 447 region denotes semi volatile species that actively partition between the gas- and particle-phases,
 448 light green denotes species that are of lower volatility, and dark green outline denotes a coating.
 449

450
 451 Another possible mechanism of organosulfate formation, as well as sulfate ester
 452 oligomers, is via S_N2 reactions where one of the 2-methyltetrol $-OH$ groups is protonated to
 453 make H_2O the leaving group while bisulfate, sulfate, or an organosulfate is the substituting group
 454 (Figure 7). At 30% RH, the particle acidity is higher due to less dilution of the sulfate, which
 455 would result in higher organosulfate concentrations and acid catalyzed accretion chemistry (Jang
 456 et al., 2002), consistent with the observation of a more prominent higher T_{\max} (lower volatility)
 457 mode compared to the 50% RH experiment. The broader higher T_{\max} mode at 50% RH indicates
 458 that there is likely an array of compounds breaking apart to give rise to this specific composition,
 459 consistent with a greater variety of oligomerization reactions occurring due to the dilution of
 460 sulfate and higher 2-methyltetrol concentrations. Previous work has identified several non-sulfur

461 containing polyol species, both monomers and oligomers, in IEPOX SOA (Surratt et al., 2010;
462 Lin et al., 2012; Lin et al., 2014).

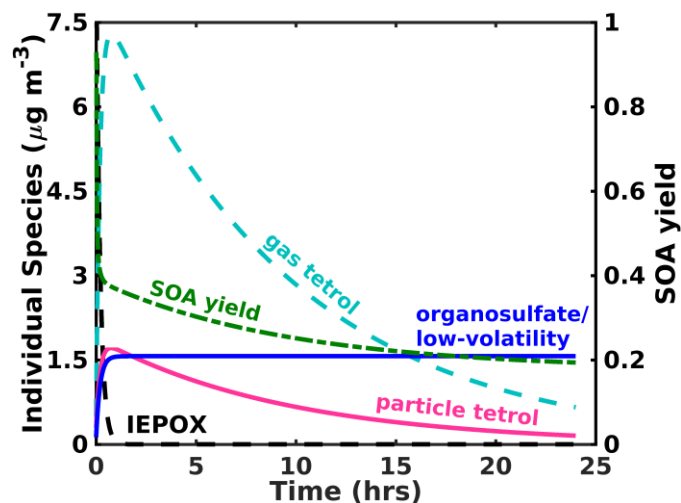
463

464 **Summary & Atmospheric Implications**

465 To place our findings into context, we present results from a simple conceptual model
466 simulating IEPOX (initially ~ 2 ppb/ $10 \mu\text{g m}^{-3}$) reactive uptake to form the corresponding 2-
467 methyltetrol and organosulfate at yields of 90 and 10%, respectively, with an uptake coefficient
468 of 0.05 based on Gaston et al. (2014), and an atmospherically relevant total surface area (2.5×10^6
469 $\text{cm}^2 \text{cm}^{-3}$) and volume ($1.6 \times 10^{-11} \text{cm}^3 \text{cm}^{-3}$). We also include a loss of gas-phase species (2-
470 methyltetrol and IEPOX) due to reaction with OH at $1.8 \times 10^{-11} \text{cm}^3 \text{molec}^{-1} \text{s}^{-1}$ (Atkinson, 1987),
471 **consistent with previous studies for the IEPOX + OH rate constant** (Bates et al., 2014; Jacobs et
472 al., 2013). The processes in the model are simplified from the reaction scheme discussed above,
473 i.e. it does not include particle-phase processes, but its purpose is to capture the salient factors
474 that control the reactive uptake and partitioning. The chosen branching between 2-methyltetrol
475 and organosulfate yields from IEPOX reactive uptake to aerosol is somewhat arbitrary and only
476 to illustrate the behavior of the system. The Henry's Law constant found via COSMOtherm for
477 the 2-methyltetrol is used to simulate gas-particle partitioning of the 2-methyltetrol, while the
478 organosulfate is a proxy for all low volatility products, including the promptly formed
479 organosulfates, sulfate esters from further accretion, and polyol oligomers. **Vapor wall loss is not**
480 **considered in the model, which might be resulting in more tetrol evaporating from the particles**
481 **in our measurements than would occur in the atmosphere. However, operating in continuous**
482 **flow mode helps to mitigate these issues, and in batch mode we do not observe a significant loss**
483 **of the low- T_{max} /semi-volatile mode. In the atmosphere, photochemical losses of the gas-phase**
484 **tetrol and the smaller aqueous volume of the aerosol would lead to partitioning of the tetrol out**
485 **of the aerosol, as illustrated by the model in Figure 8 which does include these atmospheric**
486 **processes. Thus, while vapor wall loss in the chamber potentially leads to lower particle-phase**
487 **tetrol, the chamber experiments neglect oxidation of gas-phase tetrol which would have a similar**
488 **effect in the atmosphere.**

489 The simulated loss of IEPOX and formation of IEPOX SOA are shown in Figure 8.
490 IEPOX is almost completely consumed after 1 hour of reaction, corresponding to rapid formation
491 of SOA. The composition of the aerosol changes significantly as a function of time. Initially, the
492 SOA is composed primarily of 2-methyltetrol. However, despite the relatively high Henry's law
493 constant, much of the 2-methyltetrol evaporates into the gas-phase to maintain equilibrium with
494 the gas-phase 2-methyltetrol which is subjected to loss by gas-phase bimolecular reactions with
495 the hydroxyl radical (OH). This behavior supports our findings herein that on a typical aerosol
496 lifetime, the dominant IEPOX reactive uptake product, 2-methyltetrol, will be a small component
497 of IEPOX SOA, and organosulfates and other low volatility material, including oligomers of 2-
498 methyltetrol, will dominate, albeit at a smaller overall SOA yield (Figure 8) per IEPOX reacting
499 on aerosol.

500



501 **Figure 8.** Model results for the major gas- and particle-phase species of IEPOX reactive uptake
 502 for typical atmospheric aerosol and typical IEPOX mixing ratios.
 503
 504

505 Fundamental chamber studies of IEPOX reactive uptake to aqueous acidic seed were
 506 performed and we find that the resulting molecular composition and volatility of the formed
 507 SOA confirm that the vast majority of IEPOX SOA in the atmosphere is of very low volatility, in
 508 the form of organosulfates and polyol oligomers. We show that the major product expected from
 509 IEPOX reactive uptake in acidic aqueous solutions, $C_5H_{12}O_4$ (most probably 2-methyltetrol), is
 510 semi-volatile and likely will partition out of the aerosol and thus contribute relatively little to
 511 IEPOX SOA mass under atmospheric conditions. We further confirm that the observed
 512 properties of $C_5H_{10}O_3$ are not consistent with the structure of C_5 -alkene triols and/or 3-MeTHF-
 513 3,4-diols, and thus these structures cannot be components of IEPOX SOA but are likely artifacts
 514 of thermal decomposition during analytical workup. A direct intercomparison is required to
 515 definitively determine whether all instruments are measuring the same species and that prior
 516 estimates of IEPOX SOA have not been overestimated due to “double counting” carbon in these
 517 tracers which might be derived from organosulfates and oligomers measured separately.

518 The evidence presented herein, as well as in independent experiments (Cui et al., 2018),
 519 indicates that the $C_5H_{10}O_3$, regardless of structure, as well as a significant portion of the
 520 $C_5H_{12}O_4$, are not actual components of the SOA but rather derived from other related
 521 components during the analysis. Therefore, we do not recommend that these species be included
 522 as products in mechanistic models of IEPOX SOA formation and evolution. Finally, we provide
 523 evidence that a portion of the low volatility IEPOX SOA is composed of oligomers formed in
 524 part from slower particle-phase accretion chemistry, likely involving the first generation
 525 organosulfates and possibly also the 2-methyltetrol, though we can’t distinguish between these
 526 possible combinations. The distribution of products and formation timescales depend upon
 527 aerosol water, sulfate, and hydronium ion activities, and thus ultimately on ambient RH and
 528 particle alkalinity sources. However, the low volatility of the majority of IEPOX SOA will make
 529 it less susceptible to subsequent changes in RH or dilution.

530 These findings help to explain properties of IEPOX SOA observed in the field and to
 531 resolve inconsistencies in the descriptions of IEPOX SOA formation from gas-phase IEPOX
 532 reactive uptake. The AMS IEPOX related PMF factor has been shown to correlate with sulfate
 533 (Hu et al., 2015; Xu et al., 2015). If the majority of IEPOX SOA is in the form of low volatility
 534 components, such as organosulfates and oligomers thereof as our observations indicate, then a

535 correlation of IEPOX SOA with sulfate, and not water content or acidity, is expected given the
536 direct coupling to inorganic sulfate and similar lifetimes against removal. Moreover, the low
537 SOA yield per reactive uptake of IEPOX on aqueous acidic seed can be explained as C₅H₁₂O₄,
538 the dominant product and likely 2-methyltetrol, being semi-volatile and largely partitioning out
539 of the particle-phase especially in a system with gas-phase oxidation or in chambers with vapor-
540 wall loss. Measured reactive uptake probabilities of IEPOX (γ_{IEPOX}) on aqueous acidic seed are
541 an order of magnitude or more higher than often used in models (Gaston et al., 2014; Eddingsaas
542 et al., 2010; Pye et al., 2013; Marais et al., 2016). Partly this discrepancy reflects a lower SOA
543 yield per IEPOX lost than accounted for in models, for which we provide an explanation, and
544 also a role for organic coatings that likely exist in the atmosphere which slow reactive uptake
545 relative to pure aqueous acidic seed (Gaston et al., 2014; Zhang et al., 2018).

546 These aspects likely have some cancelation of errors but could lead to errors in models of
547 IEPOX abundance and the IEPOX SOA production rate, and thus their corresponding spatial
548 variability. For example, in regions with relatively fresh, uncoated aqueous acidic particles,
549 models using a low reaction probability would underestimate the IEPOX loss rate from the gas-
550 phase, sustaining IEPOX SOA formation over a larger area than in reality. A model that ignored
551 the role of organic coatings and 2-methyltetrol evaporation would potentially overestimate
552 IEPOX SOA formation on regional scales. Models that treat products of IEPOX reactive uptake
553 in a volatility basis set would need to utilize the volatility inferred from the thermograms herein,
554 or thermal denuder measurements, rather than that inferred from commonly reported IEPOX
555 SOA tracers that utilize high-temperature analytical methods. Finally, without accounting for
556 slower accretion chemistry involving organosulfates and polyols, IEPOX SOA predicted from a
557 treatment of first generation products alone could be underestimated.

558

559 **Author Contributions**

560 E.L.D. analyzed FIGAERO data; E.L.D., J.A.T., and S.S. conducted modeling; and
561 E.L.D. and J.A.T. wrote the manuscript. J.E.S. and J.A.T. designed the chamber experiments.
562 N.H., V-T. S., G.H., and T.K. made COSMOtherm predictions. All other coauthors participated
563 in data collection, experiment operations, and manuscript discussions.

564

565

566 **Acknowledgements**

567 This work was supported by the U.S. Department of Energy ASR grants DE-SC0011791
568 and DE-SC0018221. E.L.D. was supported by the National Science Foundation Graduate
569 Research Fellowship under Grant No. DGE-1256082. PNNL authors were supported by the U.S.
570 Department of Energy, Office of Biological and Environmental Research, as part of the ASR
571 program. Pacific Northwest National Laboratory is operated for DOE by Battelle Memorial
572 Institute under contract DE-AC05-76RL01830. UC Davis authors were supported by NSF grant
573 ATM-1151062. We thank A. Gold and Z. Zhang for synthesizing the *trans*- β -IEPOX, 2-
574 methyltetrol, and 3-MeTHG-3,4-diol standards used in this work.

575

576

577

578

579 **References**

- 580 Atkinson, R.: A Structure-Activity Relationship for the Estimation of Rate Constants for the Gas-Phase
581 Reactions of OH Radicals with Organic-Compounds *Int. J. Chem. Kinet.*, **19**, 799-828,
582 10.1002/kin.550190903, 1987.
- 583 Bates, K. H., Crouse, J. D., St Clair, J. M., Bennett, N. B., Nguyen, T. B., Seinfeld, J. H., Stoltz, B. M., and
584 Wennberg, P. O.: Gas phase production and loss of isoprene epoxydiols, *J. Phys. Chem. A*, **118**,
585 1237-1246, 10.1021/jp4107958, 2014.
- 586 Bondy, A. L., Craig, R. L., Zhang, Z., Gold, A., Surratt, J. D., and Ault, A. P.: Isoprene-Derived
587 Organosulfates: Vibrational Mode Analysis by Raman Spectroscopy, Acidity-Dependent Spectral
588 Modes, and Observation in Individual Atmospheric Particles, *J. Phys. Chem. A*, **122**, 303-315,
589 10.1021/acs.jpca.7b10587, 2018.
- 590 Compornolle, S., Ceulemans, K., and Muller, J. F.: EVAPORATION: a new vapour pressure estimation
591 method for organic molecules including non-additivity and intramolecular interactions, *Atmos.*
592 *Chem. Phys.*, **11**, 9431-9450, 10.5194/acp-11-9431-2011, 2011.
- 593 Cui, T., Zeng, Z., dos Santos, E. O., Zhang, Z., Chen, Y., Zhang, Y., Rose, C. A., Budisulistiorini, S. H., Collins,
594 L. B., Bodnar, W. M., de Souza, R. A. F., Martin, S. T., Machado, C. M. D., Turpin, B. J., Gold, A.,
595 Ault, A. P., and Surratt, J. D.: Development of a hydrophilic interaction liquid chromatography
596 (HILIC) method for the chemical characterization of water-soluble isoprene epoxydiol (IEPOX)-
597 derived secondary organic aerosol, *Environmental Science: Processes & Impacts*,
598 10.1039/c8em00308d, 2018.
- 599 D'Ambro, E. L., Lee, B. H., Liu, J., Shilling, J. E., Gaston, C. J., Lopez-Hilfiker, F. D., Schobesberger, S.,
600 Zaveri, R. A., Mohr, C., Lutz, A., Zhang, Z., Gold, A., Surratt, J. D., Rivera-Rios, J. C., Keutsch, F. N.,
601 and Thornton, J. A.: Molecular composition and volatility of isoprene
602 photochemical oxidation secondary organic aerosol under low- and high-NO_x conditions, *Atmos.*
603 *Chem. Phys.*, **17**, 159-174, 10.5194/acp-17-159-2017, 2017a.
- 604 D'Ambro, E. L., Moller, K. H., Lopez-Hilfiker, F. D., Schobesberger, S., Liu, J. M., Shilling, J. E., Lee, B.,
605 Kjaergaard, H. G., and Thornton, J. A.: Isomerization of Second-Generation Isoprene Peroxy
606 Radicals: Epoxide Formation and Implications for Secondary Organic Aerosol Yields, *Environ. Sci.*
607 *Technol.*, **51**, 4978-4987, 10.1021/acs.est.7b00460, 2017b.
- 608 D'Ambro, E. L., Schobesberger, S., Zaveri, R. A., Shilling, J. E., Lee, B. H., Lopez-Hilfiker, F. D., Mohr, C.,
609 and Thornton, J. A.: Isothermal Evaporation of α -Pinene Ozonolysis SOA: Volatility, Phase State,
610 and Oligomeric Composition, *ACS Earth and Space Chemistry*,
611 10.1021/acsearthspacechem.8b00084, 2018.
- 612 Eddingsaas, N. C., VanderVelde, D. G., and Wennberg, P. O.: Kinetics and products of the acid-catalyzed
613 ring-opening of atmospherically relevant butyl epoxy alcohols, *Journal of Physical Chemistry A*,
614 **114**, 8106-8113, 10.1021/jp103907c, 2010.
- 615 Gaston, C. J., Riedel, T. P., Zhang, Z. F., Gold, A., Surratt, J. D., and Thornton, J. A.: Reactive uptake of an
616 isoprene-derived epoxydiol to submicron aerosol particles, *Environ. Sci. Technol.*, **48**, 11178-
617 11186, 10.1021/es5034266, 2014.
- 618 Guenther, A. B., Jiang, X., Heald, C. L., Sakulyanontvittaya, T., Duhl, T., Emmons, L. K., and Wang, X.: The
619 model of emissions of gases and aerosols from nature version 2.1 (MEGAN2.1): an extended and
620 updated framework for modeling biogenic emissions, *Geosci. Model Dev.*, **5**, 1471-1492,
621 10.5194/gmd-5-1471-2012, 2012.
- 622 Hallquist, M., Wenger, J. C., Baltensperger, U., Rudich, Y., Simpson, D., Claeys, M., Dommen, J., Donahue,
623 N. M., George, C., Goldstein, A. H., Hamilton, J. F., Herrmann, H., Hoffmann, T., Iinuma, Y., Jang,
624 M., Jenkin, M. E., Jimenez, J. L., Kiendler-Scharr, A., Maenhaut, W., McFiggans, G., Mentel, T. F.,
625 Monod, A., Prevot, A. S. H., Seinfeld, J. H., Surratt, J. D., Szmigielski, R., and Wildt, J.: The

626 formation, properties and impact of secondary organic aerosol: current and emerging issues,
627 *Atmos. Chem. Phys.*, 9, 5155-5236, 2009.

628 Hu, W. W., Campuzano-Jost, P., Palm, B. B., Day, D. A., Ortega, A. M., Hayes, P. L., Krechmer, J. E., Chen,
629 Q., Kuwata, M., Liu, Y. J., de Sa, S. S., McKinney, K., Martin, S. T., Hu, M., Budisulistiorini, S. H.,
630 Riva, M., Surratt, J. D., St Clair, J. M., Isaacman-Van Wertz, G., Yee, L. D., Goldstein, A. H.,
631 Carbone, S., Brito, J., Artaxo, P., de Gouw, J. A., Koss, A., Wisthaler, A., Mikoviny, T., Karl, T.,
632 Kaser, L., Jud, W., Hansel, A., Docherty, K. S., Alexander, M. L., Robinson, N. H., Coe, H., Allan, J.
633 D., Canagaratna, M. R., Paulot, F., and Jimenez, J. L.: Characterization of a real-time tracer for
634 isoprene epoxydiols-derived secondary organic aerosol (IEPOX-SOA) from aerosol mass
635 spectrometer measurements, *Atmos. Chem. Phys.*, 15, 11807-11833, 10.5194/acp-15-11807-
636 2015, 2015.

637 Hu, W. W., Palm, B. B., Day, D. A., Campuzano-Jost, P., Krechmer, J. E., Peng, Z., de Sa, S. S., Martin, S. T.,
638 Alexander, M. L., Baumann, K., Hacker, L., Kiendler-Scharr, A., Koss, A. R., de Gouw, J. A.,
639 Goldstein, A. H., Seco, R., Sjostedt, S. J., Park, J. H., Guenther, A. B., Kim, S., Canonaco, F., Prevot,
640 A. S. H., Brune, W. H., and Jimenez, J. L.: Volatility and lifetime against OH heterogeneous
641 reaction of ambient isoprene-epoxydiols-derived secondary organic aerosol (IEPOX-SOA),
642 *Atmos. Chem. Phys.*, 16, 11563-11580, 10.5194/acp-16-11563-2016, 2016.

643 Isaacman-VanWertz, G., Yee, L. D., Kreisberg, N. M., Wernis, R., Moss, J. A., Hering, S. V., de Sa, S. S.,
644 Martin, S. T., Alexander, M. L., Palm, B. B., Hu, W. W., Campuzano-Jost, P., Day, D. A., Jimenez, J.
645 L., Riva, M., Surratte, J. D., Viegas, J., Manzi, A., Edgerton, E., Baumann, K., Souza, R., Artaxo, P.,
646 and Goldstein, A. H.: Ambient Gas-Particle Partitioning of Tracers for Biogenic Oxidation,
647 *Environmental Science & Technology*, 50, 9952-9962, 10.1021/acs.est.6b01674, 2016.

648 Jacobs, M. I., Darer, A. I., and Elrod, M. J.: Rate Constants and Products of the OH Reaction with
649 Isoprene-Derived Epoxides, *Environmental Science & Technology*, 47, 12868-12876,
650 10.1021/es403340g, 2013.

651 Jang, M. S., Czoschke, N. M., Lee, S., and Kamens, R. M.: Heterogeneous atmospheric aerosol production
652 by acid-catalyzed particle-phase reactions, *Science*, 298, 814-817, 10.1126/science.1075798,
653 2002.

654 Kurtén, T., Hyttinen, N., D'Ambro, E. L., Thornton, J., and Prisle, N. L.: Estimating the saturation vapor
655 pressures of isoprene oxidation products C₅H₁₂O₆ and C₅H₁₀O₆ using COSMO-RS, *Atmos.*
656 *Chem. Phys.*, 18, 17589-17600, 10.5194/acp-18-17589-2018, 2018.

657 Lee, B. H., Lopez-Hilfiker, F. D., Mohr, C., Kurten, T., Worsnop, D. R., and Thornton, J. A.: An iodide-
658 adduct high-resolution time-of-flight chemical-ionization mass spectrometer: application to
659 atmospheric inorganic and organic compounds, *Environ. Sci. Technol.*, 48, 6309-6317,
660 10.1021/es500362a, 2014.

661 Lin, Y. H., Zhang, Z. F., Docherty, K. S., Zhang, H. F., Budisulistiorini, S. H., Rubitschun, C. L., Shaw, S. L.,
662 Knipping, E. M., Edgerton, E. S., Kleindienst, T. E., Gold, A., and Surratt, J. D.: Isoprene epoxydiols
663 as precursors to secondary organic aerosol formation: Acid-catalyzed reactive uptake studies
664 with authentic compounds, *Environ. Sci. Technol.*, 46, 250-258, 10.1021/es202554c, 2012.

665 Lin, Y. H., Budisulistiorini, H., Chu, K., Siejack, R. A., Zhang, H. F., Riva, M., Zhang, Z. F., Gold, A.,
666 Kautzman, K. E., and Surratt, J. D.: Light-absorbing oligomer formation in secondary organic
667 aerosol from reactive uptake of isoprene epoxydiols, *Environ. Sci. Technol.*, 48, 12012-12021,
668 10.1021/es503142b, 2014.

669 Liu, J. M., D'Ambro, E. L., Lee, B. H., Lopez-Hilfiker, F. D., Zaveri, R. A., Rivera-Rios, J. C., Keutsch, F. N.,
670 Iyer, S., Kurten, T., Zhang, Z. F., Gold, A., Surratt, J. D., Shilling, J. E., and Thornton, J. A.: Efficient
671 isoprene secondary organic aerosol formation from a non-IEPOX pathway, *Environ. Sci. Technol.*,
672 50, 9872-9880, 10.1021/acs.est.6b01872, 2016.

673 Liu, S., Shilling, J. E., Song, C., Hiranuma, N., Zaveri, R. A., and Russell, L. M.: Hydrolysis of organonitrate
674 functional groups in aerosol particles, *Aerosol Sci. Technol.*, 46, 1359-1369,
675 10.1080/02786826.2012.716175, 2012.

676 Lopez-Hilfiker, F. D., Mohr, C., Ehn, M., Rubach, F., Kleist, E., Wildt, J., Mentel, T. F., Lutz, A., Hallquist,
677 M., Worsnop, D., and Thornton, J. A.: A novel method for online analysis of gas and particle
678 composition: description and evaluation of a Filter Inlet for Gases and AEROSols (FIGAERO),
679 *Atmos. Meas. Tech.*, 7, 983-1001, 10.5194/amt-7-983-2014, 2014.

680 Lopez-Hilfiker, F. D., Mohr, C., D'Ambro, E. L., Lutz, A., Riedel, T. P., Gaston, C. J., Iyer, S., Zhang, Z., Gold,
681 A., Surratt, J. D., Lee, B. H., Kurten, T., Hu, W. W., Jimenez, J., Hallquist, M., and Thornton, J. A.:
682 Molecular composition and volatility of organic aerosol in the southeastern US: Implications for
683 IEPOX derived SOA, *Environ. Sci. Technol.*, 50, 2200-2209, 10.1021/acs.est.5b04769, 2016.

684 Marais, E. A., Jacob, D. J., Jimenez, J. L., Campuzano-Jost, P., Day, D. A., Hu, W., Krechmer, J., Zhu, L.,
685 Kim, P. S., Miller, C. C., Fisher, J. A., Travis, K., Yu, K., Hanisco, T. F., Wolfe, G. M., Arkinson, H. L.,
686 Pye, H. O. T., Froyd, K. D., Liao, J., and McNeill, V. F.: Aqueous-phase mechanism for secondary
687 organic aerosol formation from isoprene: application to the southeast United States and co-
688 benefit of SO₂ emission controls, *Atmos. Chem. Phys.*, 16, 1603-1618, 10.5194/acp-16-1603-
689 2016, 2016.

690 Paulot, F., Crouse, J. D., Kjaergaard, H. G., Kurten, A., St Clair, J. M., Seinfeld, J. H., and Wennberg, P. O.:
691 Unexpected epoxide formation in the gas-phase photooxidation of isoprene, *Science*, 325, 730-
692 733, 10.1126/science.1172910, 2009.

693 Pye, H. O. T., Pinder, R. W., Piletic, I. R., Xie, Y., Capps, S. L., Lin, Y. H., Surratt, J. D., Zhang, Z. F., Gold, A.,
694 Luecken, D. J., Hutzell, W. T., Jaoui, M., Offenberg, J. H., Kleindienst, T. E., Lewandowski, M., and
695 Edney, E. O.: Epoxide pathways improve model predictions of isoprene markers and reveal key
696 role of acidity in aerosol formation, *Environmental Science & Technology*, 47, 11056-11064,
697 10.1021/es402106h, 2013.

698 Riedel, T. P., Lin, Y. H., Budisulistiorini, H., Gaston, C. J., Thornton, J. A., Zhang, Z. F., Vizuete, W., Gold, A.,
699 and Surratt, J. D.: Heterogeneous reactions of isoprene-derived epoxides: reaction probabilities
700 and molar secondary organic aerosol yield estimates, *Environ. Sci. Technol. Lett.*, 2, 38-42,
701 10.1021/ez500406f, 2015.

702 Riva, M., Budisulistiorini, S. H., Chen, Y. Z., Zhang, Z. F., D'Ambro, E. L., Zhang, X., Gold, A., Turpin, B. J.,
703 Thornton, J. A., Canagaratna, M. R., and Surratt, J. D.: Chemical characterization of secondary
704 organic aerosol from oxidation of isoprene hydroxyhydroperoxides, *Environ. Sci. Technol.*, 50,
705 9889-9899, 10.1021/acs.est.6b02511, 2016.

706 Schobesberger, S., D'Ambro, E. L., Lopez-Hilfiker, F. D., Mohr, C., and Thornton, J. A.: A model framework
707 to retrieve thermodynamic and kinetic properties of organic aerosol from composition-resolved
708 thermal desorption measurements, *Atmos. Chem. Phys.*, 18, 14757-14785, 10.5194/acp-18-
709 14757-2018, 2018.

710 St Clair, J. M., Rivera-Rios, J. C., Crouse, J. D., Knap, H. C., Bates, K. H., Teng, A. P., Jørgensen, S.,
711 Kjaergaard, H. G., Keutsch, F. N., and Wennberg, P. O.: Kinetics and products of the reaction of
712 the first-generation isoprene hydroxy hydroperoxide (ISOPOOH) with OH, *Journal of Physical
713 Chemistry A*, 120, 1441-1451, 10.1021/acs.jpca.5b06532, 2016.

714 Surratt, J. D., Murphy, S. M., Kroll, J. H., Ng, N. L., Hildebrandt, L., Sorooshian, A., Szmigielski, R.,
715 Vermeylen, R., Maenhaut, W., Claeys, M., Flagan, R. C., and Seinfeld, J. H.: Chemical composition
716 of secondary organic aerosol formed from the photooxidation of isoprene, *Journal of Physical
717 Chemistry A*, 110, 9665-9690, 10.1021/jp061734m, 2006.

718 Surratt, J. D., Kroll, J. H., Kleindienst, T. E., Edney, E. O., Claeys, M., Sorooshian, A., Ng, N. L., Offenberg, J.
719 H., Lewandowski, M., Jaoui, M., Flagan, R. C., and Seinfeld, J. H.: Evidence for organosulfates in
720 secondary organic aerosol, *Environ. Sci. Technol.*, 41, 517-527, 10.1021/es062081q, 2007a.

721 Surratt, J. D., Lewandowski, M., Offenberg, J. H., Jaoui, M., Kleindienst, T. E., Edney, E. O., and Seinfeld, J.
722 H.: Effect of acidity on secondary organic aerosol formation from isoprene, *Environ. Sci.*
723 *Technol.*, 41, 5363-5369, 10.1021/es0704176, 2007b.

724 Surratt, J. D., Chan, A. W. H., Eddingsaas, N. C., Chan, M. N., Loza, C. L., Kwan, A. J., Hersey, S. P., Flagan,
725 R. C., Wennberg, P. O., and Seinfeld, J. H.: Reactive intermediates revealed in secondary organic
726 aerosol formation from isoprene, *Proc. Natl. Acad. Sci. U. S. A.*, 107, 6640-6645,
727 10.1073/pnas.0911114107, 2010.

728 Wang, W., Kourtchev, I., Graham, B., Cafmeyer, J., Maenhaut, W., and Claeys, M.: Characterization of
729 oxygenated derivatives of isoprene related to 2-methyltetrols in Amazonian aerosols using
730 trimethylsilylation and gas chromatography/ion trap mass spectrometry, *Rapid Commun. Mass*
731 *Spectrom.*, 19, 1343-1351, 10.1002/rcm.1940, 2005.

732 Watanabe, A. C., Stropoli, S. J., and Elrod, M. J.: Assessing the Potential Mechanisms of Isomerization
733 Reactions of Isoprene Epoxydiols on Secondary Organic Aerosol, *Environ. Sci. Technol.*, 52, 8346-
734 8354, 10.1021/acs.est.8b01780, 2018.

735 Waxman, E. M., Elm, J., Kurtén, T., Mikkelsen, K. V., Ziemann, P. J., and Volkamer, R.: Glyoxal and
736 Methylglyoxal Setschenow Salting Constants in Sulfate, Nitrate, and Chloride Solutions:
737 Measurements and Gibbs Energies, *Environ. Sci. Technol.*, 49, 11500-11508,
738 10.1021/acs.est.5b02782, 2015.

739 Xu, L., Guo, H. Y., Boyd, C. M., Klein, M., Bougiatioti, A., Cerully, K. M., Hite, J. R., Isaacman-VanWertz, G.,
740 Kreisberg, N. M., Knote, C., Olson, K., Koss, A., Goldstein, A. H., Hering, S. V., de Gouw, J.,
741 Baumann, K., Lee, S. H., Nenes, A., Weber, R. J., and Ng, N. L.: Effects of anthropogenic emissions
742 on aerosol formation from isoprene and monoterpenes in the southeastern United States, *Proc.*
743 *Natl. Acad. Sci. U. S. A.*, 112, 37-42, 10.1073/pnas.1417609112, 2015.

744 Zhang, Y., Chen, Y., Lambe, A. T., Olson, N. E., Lei, Z., Craig, R. L., Zhang, Z., Gold, A., Onasch, T. B., Jayne,
745 J. T., Worsnop, D. R., Gaston, C. J., Thornton, J. A., Vizuete, W., Ault, A. P., and Surratt, J. D.:
746 Effect of the Aerosol-Phase State on Secondary Organic Aerosol Formation from the Reactive
747 Uptake of Isoprene-Derived Epoxydiols (IEPOX), *Environ. Sci. Technol. Lett.*, 5, 167-174,
748 10.1021/acs.estlett.8b00044, 2018.

749 Zhang, Z., Lin, Y. H., Zhang, H., Surratt, J. D., Ball, L. M., and Gold, A.: Technical Note: Synthesis of
750 isoprene atmospheric oxidation products: isomeric epoxydiols and the rearrangement products
751 *cis*- and *trans*-3-methyl-3,4-dihydroxytetrahydrofuran, *Atmos. Chem. Phys.*, 12, 8529-8535,
752 10.5194/acp-12-8529-2012, 2012.

753